



HAL
open science

Cyclopentadienyl/Fluorenyl-Group 4 ansa-metallocene Catalysts for Production of Tailor-made Polyolefins

Evgueni Kirillov, Jean-François Carpentier

► **To cite this version:**

Evgueni Kirillov, Jean-François Carpentier. Cyclopentadienyl/Fluorenyl-Group 4 ansa-metallocene Catalysts for Production of Tailor-made Polyolefins. *Chemical Record*, 2021, 21 (2), pp.357-375. 10.1002/tcr.202000142 . hal-03102146

HAL Id: hal-03102146

<https://hal.science/hal-03102146>

Submitted on 4 Feb 2021

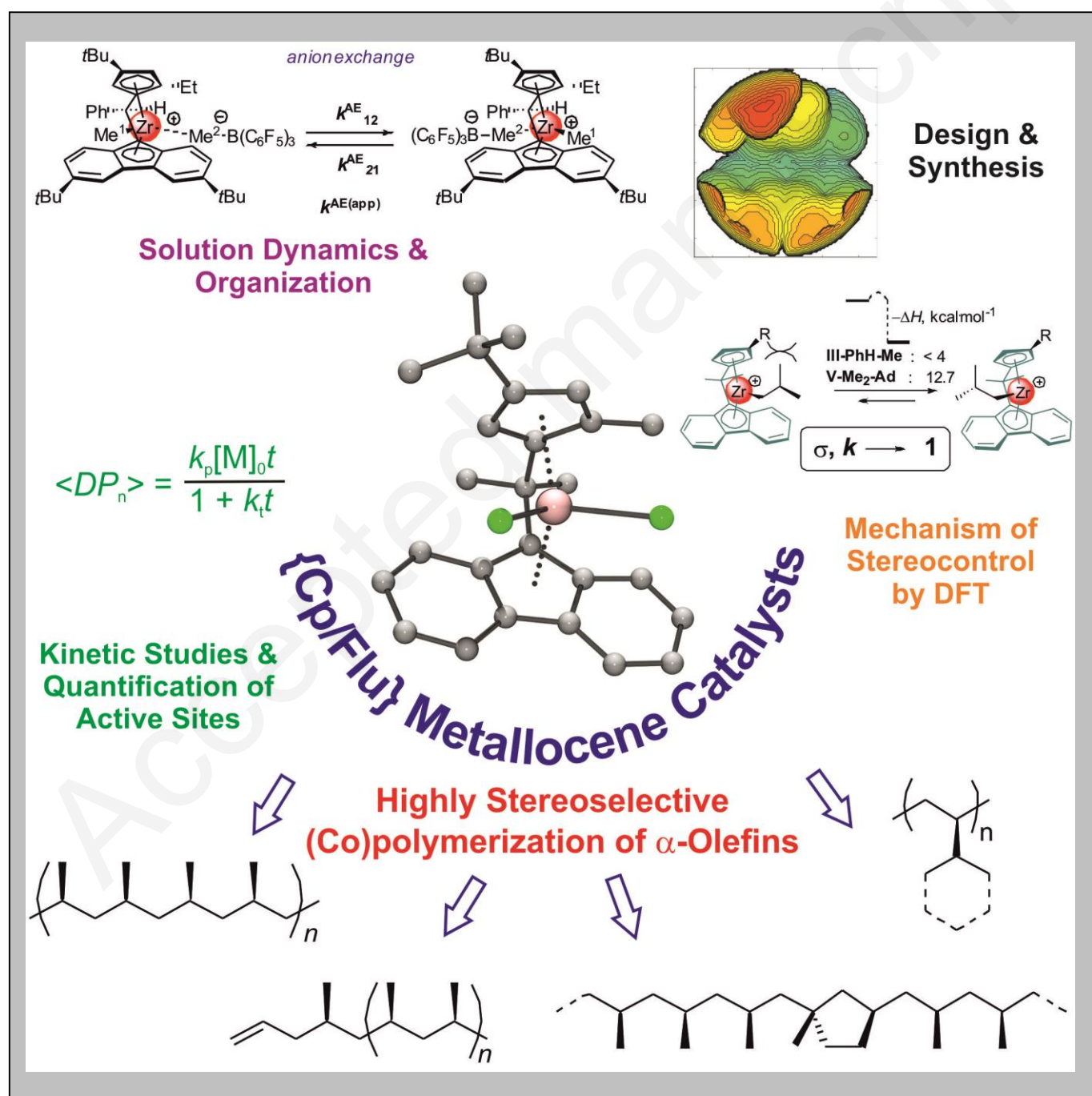
HAL is a multi-disciplinary open access archive for the deposit and dissemination of scientific research documents, whether they are published or not. The documents may come from teaching and research institutions in France or abroad, or from public or private research centers.

L'archive ouverte pluridisciplinaire **HAL**, est destinée au dépôt et à la diffusion de documents scientifiques de niveau recherche, publiés ou non, émanant des établissements d'enseignement et de recherche français ou étrangers, des laboratoires publics ou privés.

{Cyclopentadienyl/Fluorenyl}-Group 4 *ansa*-Metallocene Catalysts for Production of Tailor-Made Polyolefins

Evgueni Kirillov^{*[a]} and Jean-François Carpentier^{*[a]}

Dedication: dedicated to the memories of Prof. Malcolm H. Green, deceased July 24, 2020 and Prof. André Mortreux, deceased October 10, 2020.



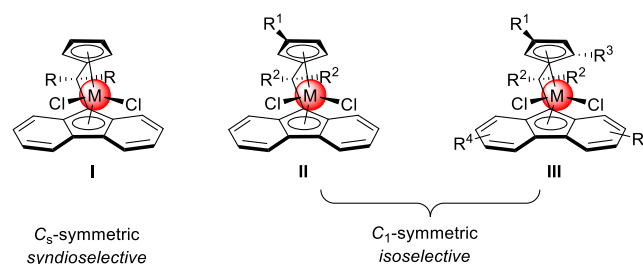
Abstract: The development of new metallocene-based polymerization catalysts and innovative processes derived thereof still constitutes a challenge for the manufacturing of polyolefinic materials with tailored properties (e.g. particular microstructure or topology, ultra-high molecular weight, high melting transition, and their combinations) for contemporary commercial applications. This personal account summarizes our continuing endeavors to advance the family of industry-relevant stereoselective propylene polymerization catalysts based on C_1 -symmetric group 4 *ansa*-metallocenes incorporating multi-substituted fluorenyl-cyclopentadienyl {Cp/Flu} ligands. Within the framework of this project, valuable structural and catalytic data, harvested both for neutral metallocenes and for metallocenium ion-pairs, have been used for rational design of more efficient catalytic systems, reluctant towards side reactions, and for providing new stereoregular value-added polymer materials.

1. Introduction

In the first half of the 20th century, the first large-scale commercial polymers were produced either by free radical polymerization (low density polyethylene (LDPE), poly(vinyl chloride), polystyrene, poly(methyl methacrylate)) or polycondensation reactions (polyamides, polyesters, etc.).^[1] These polymerizations afforded materials with none to low crystallinity, and the question of polymerization stereocontrol – when relevant – was largely disregarded, since even the concept of macromolecules was fairly new at the time. With the discovery of metal-catalyzed olefin polymerization in 1950s by K. Ziegler and G. Natta, the first crystalline polyolefins, namely high-density polyethylene (HDPE) and isotactic polypropylene (iPP), rapidly overwhelmed the plastics markets. Since the advent of metallocene olefin polymerization catalysis in 1980s, known as “metallocene revolution”, this realm has witnessed an impressive growth in subsequent decades.^[2] The nowadays well-established direct relationship between polymer properties and structure of the metallocene catalyst has allowed the production of tailor-made, well-defined polymers. The polymerization control of metallocene-based catalytic systems makes possible the design of more complex polyolefin-based materials with enhanced properties.^[3] In addition, the solubility of single-site catalysts makes easier their studies using spectroscopic methods. Therefore, metallocene systems are excellent models for studying polymerization active sites and they have unveiled many mechanistic aspects pertaining to main steps of the coordination/insertion polymerization mechanism. So long as metallocene catalysts have revealed a range of unique features (e.g. single-site behavior, exceptional structure tunability, extremely high activity) over conventional (admittedly more cost-advantageous) Ziegler-Natta catalysts, their eventual involvement in industrial processes

added a new dimension to the production of commercial polyolefin materials.^[4] Among them, there are such products as commodity high-density polyethylene (HDPE) and iPP, specialty syndiotactic polypropylene (sPP) and high-performance specialty ultra-high molecular weight polyethylene (UHMWPE).^[5]

Isotactic polypropylene (iPP) is one of the leading and still fast-growing thermoplastic polymers in the world due to its high melting point, high tensile strength, stiffness, reusability and chemical resistance. The superior properties of the commercially metallocene-produced polypropylene (mPP) grades are valuable in certain end-use market segments, especially for high melt strength fibers and injection molded parts. These materials are largely utilized in medical, food, consumer and industrial packaging and automotive applications.^[4] Amongst the great number of industrially relevant metallocene-based polymerization catalysts,^{[1],[2]} group 4 *ansa*-metallocenes supported by bridged cyclopentadienyl-fluorenyl ({Cp/Flu}) ligand platforms hold a strikingly unique position.^[6] Originally designed by Razavi and Ewen at Fina Oil, this family of single-site metallocene catalysts has proven especially valuable for stereoselective polymerization of α -olefins.^[7] The high tunability of {Cp/Flu} ligands allows the introduction of various substituents at different positions of the Cp, Flu and bridge moieties, and therefore access to a class of catalysts that can combine high catalytic activity/productivity, excellent control and notably remarkable stereoselectivity in α -olefin (co)polymerization, essentially of propylene. For instance, in the series of one-carbon bridged systems, C_s -symmetric precatalysts (Scheme 1, **I-R₂**) were shown to produce highly syndiotactic polypropylene ($[r]^4 > 75\%$, where r stands for a *racemo* diad, i.e. enchainment of two monomer units) under both homogeneous and heterogeneous conditions. Modification of the ligand skeleton in the precatalyst, namely installation of a bulky substituent R¹ (*t*Bu) that imposes an overall C_1 -symmetry of the metallocene molecule (Scheme 1, **II-R¹-R²** and **III-R¹-R²-R³-R⁴**), resulted in highly isoselective systems for polymerization of propylene ($[m]^4 > 79\%$, where m stands for a *meso* diad). The fact that such a simple adjustment of the metal coordination sphere enabled dramatic changes in the stereocontrol mechanism of propylene polymerization has opened up a rich domain of investigations aiming at establishing and rationalizing the structure-activity-properties relationships in these {Cp/Flu} metallocene systems.^{[8],[9],[10]}



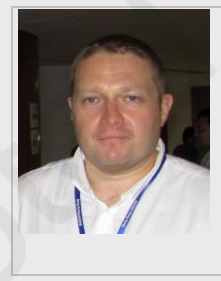
Scheme 1. Main classes of stereoselective {Cp/Flu} metallocene catalysts

[a] Evgueni Kirillov, Jean-François Carpentier
 Organometallics : Materials & Catalysis
 Institut des Sciences Chimiques de Rennes (ISCR)
 UMR 6226 CNRS – Univ Rennes
 Campus de Beaulieu
 F-35042 Rennes, France
 E-mail: evgueni.kirillov@univ-rennes1.fr,
 jean-francois.carpentier@univ-rennes1.fr

While syndiotactic polypropylene (sPP) has found only a relatively small niche on the plastics market, its congener – isotactic polypropylene (iPP) – is one of the landmarks with a global production of more than 50 MT/y. Besides heterogeneous Ziegler-Natta catalytic systems, single-site group 4 metallocene systems in homogeneous or, most preferably, in heterogenized silica-supported forms are also intensively used for the production of iPP and iPP-based olefinic copolymers. Zirconocenes belonging to the two main families, namely C_2 -symmetric silicon-bridged *ansa*-bis(indenyl) ($\{R^1_2Si-(2-Me-4-R^2-Ind)_2\}$ commonly referred to as {SBI} (e.g., *rac*- $\{Me_2Si-(2-Me-4-Ph-Ind)_2\}ZrCl_2$ ({SBI}-1)), and C_1 -symmetric one-carbon-bridged cyclopentadienyl-fluorenyl ($\{R_2C-(Flu)(Cp)\}$ or {Cp/Flu} complexes (Scheme 1, **II**- $R^1-R^2_2$ and **III**- $R^1-R^2_2-R^3-R^4$), respectively, are largely applied in industry for isoselective propylene (co)polymerization.^[11]

In the early 2000s, we initiated a project with industry aimed at elaborating more efficient catalytic systems for stereoselective polymerization of α -olefins based on {Cp/Flu}-type group 4 metallocene complexes. Thus, this account summarizes the results on the design and synthesis of new metallocene catalysts, and their evaluation in propylene polymerization catalysis. Also, a particular emphasis of the work was placed on understanding the role of steric and electronic factors on the global efficiency of metallocene catalysts (in terms of productivity and characteristics of polymer products), investigations of structure, dynamics and stability of active species, as well as determination of crucial kinetic parameters to sketch the overall activation and polymerization mechanism.

Evgueni Kirillov obtained his B.S./M.S. degree from Nizhny Novgorod State University (1996) and Ph.D. degree from G.A. Razuvaev Institute of Organometallic Chemistry of Russian Academy of Sciences (2000) with Mikhail N. Bochkarev. He conducted postdoctoral studies with Jean-François Carpentier (University of Rennes 1) and with John A. Gladysz (Friedrich Alexander Universität Erlangen-Nürnberg). He completed his habilitation (HDR) in 2008 and since 2009 he holds an appointment as Associate Professor at the University of Rennes 1. His main current research interests include the organometallic chemistry with applications in the polymerization catalysis, fine chemicals reactions and catalytic fixation of CO_2 . He has coauthored >100 papers, patents, and book chapters.



J.-F. Carpentier is 53. He graduated from the Chemical Engineering School of Lille, France, in 1989 and received his Ph. D. in molecular catalysis from the University of Lille in 1992 under the guidance of Pr. André Mortreux. In 1993 he took up a CNRS research fellow position, working on late transition metal catalysis. In 1997, he spent one year as research associate with Pr. Richard F. Jordan at the University of Iowa, working on group 4 metal d^0 -olefin complexes. In 2001, he moved to the University of Rennes as full Professor. His main



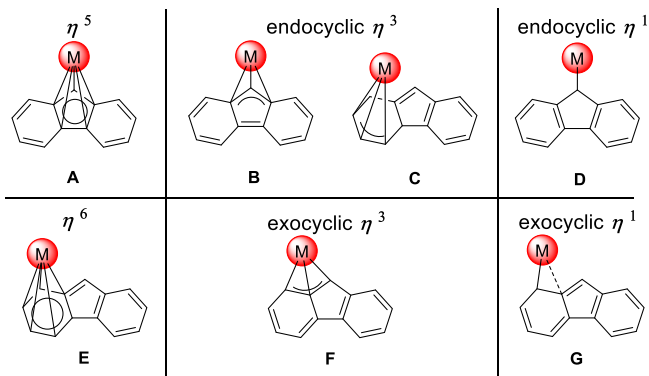
research interests lie in the organometallic chemistry of oxophilic elements and their use in catalysis for polymer materials engineering and fine chemicals synthesis. He has coauthored 340 international publications and 71 patent families. He is/was a member of several editorial boards (*Chem. Eur. J.*, *Curr. Inorg. Chem.*, *Eur. J. Inorg. Chem.*, *Organometallics*, *Polymers*); he is editor of *Catalysis Communications* since 2012. In 2005, he was elected member of the Institut Universitaire de France. In 2014, he was awarded the Silver CNRS medal and the prix Germaine & André Lequeux from the French Academy of Sciences. Besides, since April 2016, he acts as vice-president in charge of research of the Université de Rennes 1.

2. C_1 -Symmetric Metallocene Catalysts Incorporating {Cp/Flu} Ligands

2.1. Coordination Diversity of Fluorenyl-Based Ligand Platforms

The versatile bonding potential of fluorenyl ligand is obvious from the surprisingly large variety of coordination modes observed in complexes of both transition and *p*-block metals (Scheme 2).^{[6a],[12]} Those corresponding to type **A** (η^5) and type **B** (η^3) are by far the most common, that is essentially electronic in origin.^[12] In particular, the bridgehead carbon accommodating the HOMO orbital is, in general, bound to a metal atom much more strongly than the other fluorenyl atoms. As a consequence, type **A** coordination often shows a clear tendency to asymmetry, with a metal slippage towards the bridgehead atom, *i.e.* towards type **B** η^3 coordination and even further towards type **D** η^1 coordination. This suggests that the energy surface of the pathways connecting types **A**, **B** and **D** can be particularly flat.^[13] Therefore, minute perturbations, such as steric interactions or solvation effects, may facilitate (reversible) $\eta^5 \leftrightarrow \eta^3 \leftrightarrow \eta^1$ haptotropic rearrangements. This variety of readily available coordination modes in fluorenyl ligands provides opportunities in catalysis to control the coordination sphere and “as-needed” saturation of the metal center, and the overall geometry and reactivity of active species.

Also, the whole series of *ansa*-metallocenes incorporating one-carbon bridged {Cp/Flu} ligand systems has a common structural feature, that is very narrow $Cp_{cent}-M-Flu_{cent}$ bite angles. This parameter not only determines the primary coordination sphere of the metal center, but can also greatly affect its electronic properties and, therefore, its reactivity.

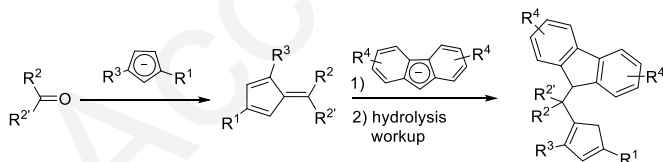


Scheme 2. Coordination modes of fluorenyl ligands observed in complexes of various metals.^[12]

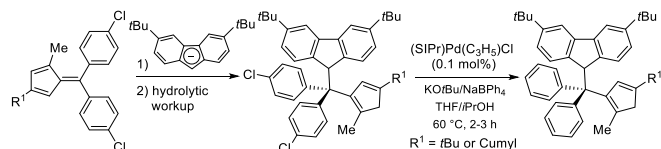
2.2. Ligand Design Concept and Synthesis of Metallocene Complexes

Another crucial feature of this class of catalysts is the remarkable influence of the distal substituents R^{1-4} in the {Cp/Flu} ligand platform on the catalytic productivity, as well as regio- and stereoselectivity and molecular weight characteristics of the resulting iPP. Thus, a number of modifications were scrutinized: (1) variation of the bulkiness of the R^1 and R^3 substituents at the Cp ligand, (2) replacement of methyl groups in the reference system **III** with phenyl or H groups in the R^2R^2C bridge, (3) variation of the nature and steric hindrance of the substituents R^4 at the Flu platform.

Nucleophilic addition of cyclopentadienyl-type anions to fulvenes has proven to be the most versatile and efficient route for the synthesis of one-carbon-bridged bis(cyclopentadienyl) and related ligands.^[14] In our studies, a variety of fluorenyl-cyclopentadienyl type ligands was prepared via this procedure (Scheme 3).^{[15],[16],[17]} In a few cases, when the more sterically crowded fulvenes incorporating $R^2, R^2 = Ph$ and $R^3 = Me$ were found reluctant towards nucleophilic addition of the [3,6-*t*Bu₂Flu]⁻ anion under a variety of conditions, an alternative protocol was elaborated (Scheme 4). In that case, the use of more electrophilic fulvenes incorporating chloro activating groups in the 4-phenyl positions appeared crucial to achieve selective nucleophilic addition of the fluorenyl anion and allowed their subsequent selective removal via a Pd-catalyzed reductive dechlorination, to eventually yield the diphenylmethylene-bridged pro-ligands.

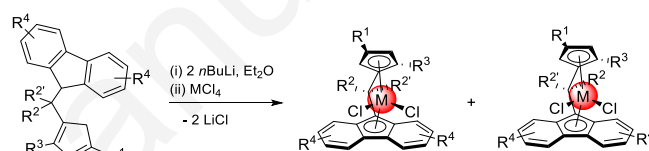


Scheme 3. General synthesis of fulvenes and proligands {Cp/Flu}H₂.



Scheme 4. Synthesis of constrained Ph₂C-bridged proligands {Ph₂C(3,6-*t*Bu₂Flu)(3-*R*¹-5-MeC₅H₂)H₂} (SIPr stands for 1,3-bis(2,6-diisopropylphenyl)imidazol-2-ylidene).

Ansa-dichlorometallocene complexes were prepared from MCl₄ (M = Zr, Hf) and the corresponding ligand dianions, generated in situ via addition of 2 equiv of *n*-butyllithium to the proligand, using a regular salt metathesis protocol in diethyl ether (Scheme 5). After workup and a recrystallization step, analytically pure dichlorometallocenes could be isolated, generally in good yields. Thus, in the framework of our studies, more than 20 new metallocene complexes were obtained (Scheme 6), which can be sorted into three types differing by the substitution patterns on the fluorenyl fragment: **III** – 3,6- R^4_2 ; **IV** – 2,7- R^4_2 and **V** – R^4_2 = octamethyloctahydrodibenzofluorenyl.

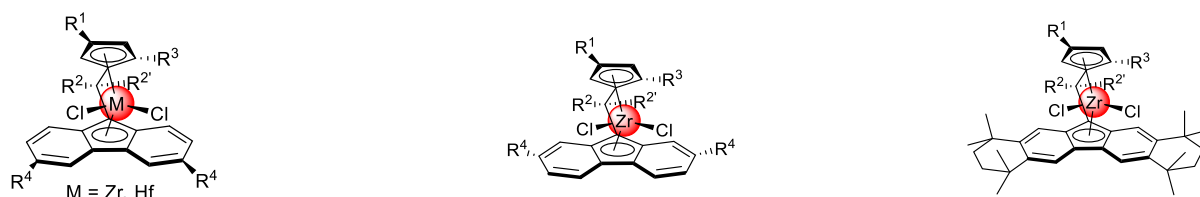


Scheme 5. Syntheses of *ansa*-metallocene complexes (M = Zr, Hf; when relevant ($R^2 \neq R^2$), only one enantiomer is depicted for each diastereomer).

2.3. About Structural and Electronic Features of Neutral Metallocene Complexes

Different descriptors have been used in the literature for a better representation of the overall structure, steric hindrance around the metal center and coordination patterns of cyclopentadienyl and related ligand systems in metallocene complexes; this includes notably, as aforementioned, Cp ligand ring slippage from ideal η^5 coordination (tentatively estimated as a relative difference in the M–C(Cp ring) distances), Cp_{cent}–M–Cp'_{cent} bite angle or, more recently, the percentage of buried volume, %V_{bur}.^[18] Also, theoretical calculations have been employed on a regular basis, providing valuable information both on their presumed structures in gas-phase or in solution (with an appropriate solution model) and on electronic properties (e.g. Natural Population Analysis (NPA) charges) of metallocene complexes, especially for those complexes whose X-ray diffraction structural data could not be obtained (e.g. **III-Ph₂-Me** or Ph₂Si-bridged **Si-IV-Ph₂-Me**).

In the solid state, all zirconocene dichlorides incorporating R₂C-bridged {Cp/Flu} ligands exhibited geometrical parameters essentially similar, as described by several other groups.^{[7b],[8a,b]} In most complexes, the coordination mode of the central five-membered ring of the fluorenyl ligand deviates slightly from η^5 towards η^3 , as evidenced by the significant differences in the M–C(ring) distances (ca. 0.3 Å between the shortest and the



| Complex | R ¹ | R ² /R ^{2'} | R ³ | R ⁴ |
|--|----------------------------|---------------------------------|----------------|----------------|
| II-PhH-Me | <i>t</i> Bu | Ph/H | Me | H |
| III-H₂-Me | <i>t</i> Bu | H/H | Me | <i>t</i> Bu |
| III-Me₂-Me | <i>t</i> Bu | Me/Me | Me | <i>t</i> Bu |
| III-Ph₂-Me | <i>t</i> Bu | Ph/Ph | Me | <i>t</i> Bu |
| III-Cumyl-Ph₂ | Cumyl | Ph/Ph | Me | <i>t</i> Bu |
| III-PhH-Me | <i>t</i> Bu | Ph/H | Me | <i>t</i> Bu |
| III-PhH-Et | <i>t</i> Bu | Ph/H | Et | <i>t</i> Bu |
| III-PhH-Ph | <i>t</i> Bu | Ph/H | Ph | <i>t</i> Bu |
| III-Ph₂ | <i>t</i> Bu | Ph/Ph | H | <i>t</i> Bu |
| III-Bu₃-Ph₂ | <i>n</i> Bu ₃ C | Ph/Ph | H | <i>t</i> Bu |

| Complex | R ¹ | R ² /R ^{2'} | R ³ | R ⁴ |
|---|----------------------------|---------------------------------|----------------|----------------|
| IV-Ph₂-Me | <i>t</i> Bu | Ph/Ph | Me | <i>t</i> Bu |
| IV-PhH-Me | <i>t</i> Bu | Ph/H | Me | <i>t</i> Bu |
| IV-Bu₃-Ph₂ | <i>n</i> Bu ₃ C | Ph/Ph | H | <i>t</i> Bu |
| IV-Ph₂-Cumyl | <i>t</i> Bu | Ph/Ph | H | Cumyl |
| IV-Ph₂-Mes | <i>t</i> Bu | Ph/Ph | H | Mesityl |
| Si-IV-Ph₂-Me | <i>t</i> Bu | Ph/Ph | Me | <i>t</i> Bu |

| Complex | R ¹ | R ² /R ^{2'} | R ³ |
|-------------------------|----------------|---------------------------------|----------------|
| V-PhH-Me | <i>t</i> Bu | Ph/H | Me |
| V-PhH-Et | <i>t</i> Bu | Ph/H | Et |
| V-Ph₂ | <i>t</i> Bu | Ph/Ph | H |

Scheme 6. Series of C₁-symmetric {Cp/Flu} ansa-metalloocene complexes (only one enantiomer is shown).^{[15],[16],[17]}

longest bond lengths). This reduced coordination hapticity ($\eta^5 \rightarrow \eta^3$) is apparently maintained in solution, since the ¹³C NMR spectroscopic studies revealed particularly upfield chemical shifts for the C9-fluorenyl carbon signals (δ_c 70.3–77.9 ppm).^[19] The Cp_{cent}–Zr–Flu_{cent} bite angles in the R₂C-bridged metallocene complexes were generally found in a quite narrow range of values (117.8–118.7 °) and compare well with the corresponding value in the prototype Me₂C-bridged metallocene III-Me₂-Me (118.5(3) °).^[7b,c] The computed %V_{bur} data provide a measurement of the space occupied by the ligand in the first coordination sphere of the metal center and steric maps were generated for a selected series of complexes (Scheme 7).

Despite the numerous structural and computational data thus collected, their direct comparison and rationalization still remains a difficult task. A few trends can be drawn for short series of closely related structures, which tentatively could be extended to a larger series of {Cp/Flu} metallocene molecules:

1) Changing the substitution pattern in the Flu ligand from 3,6-*t*Bu₂- to 2,7-*t*Bu₂- did not affect significantly either %V_{bur} or NPA charge values within the series **III-IV-PhH-Me**; however, introduction of the octamethyloctahydrodibenzofluorenyl platform (**V-PhH-Me**) significantly modified both parameters.

2) Replacing Zr by Hf in **III-PhH-Me** resulted in a more electron-rich metal center (in terms of NPA charge), whereas such

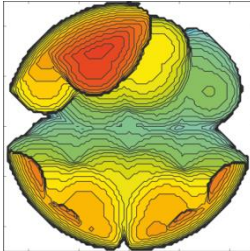
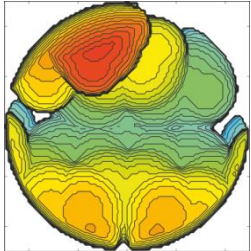
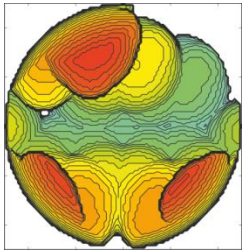
structural features as the Cp_{cent}–Zr–Flu_{cent} bite angles and %V_{bur} were not much affected (as a result of the similar sizes of these metal centers).^[20]

3) Within the series **III-R₂-Me**, when the bridge substitution pattern R²R^{2'}C was varied as H₂C → Me₂C → PhHC, mostly the electronic properties of the metal center (NPA charge) were influenced and, only slightly, the first coordination sphere (%V_{bur}).

4) Installation of a more sterically congested Ph₂C- bridge (**IV-Ph₂-Me** vs **IV-PhH-Me**) reduced the coordination sphere of the metal center (in terms of %V_{bur}), but the Cp_{cent}–Zr–Flu_{cent} bite angle and NPA charge remained almost unchanged.

5) The most drastic effect affecting all the calculated parameters was identified for the metallocene molecule **Si-IV-Ph₂-Me** incorporating a larger silylene-bridge. The larger %V_{bur} and Cp_{cent}–Zr–Flu_{cent} bite angle values are in line with the significant reduction of the coordination sphere, and the smaller NPA charge value is diagnostic of the poorer electron density on the metal center.

| | | |
|--|------------------------------|--|
| | III-H₂-Me | |
| V _{bur} , [%] | 58.4 | |
| (Cp _{cent} –M–Flu _{cent} bite angle [°]) | (118.08) | |
| NPA charge on M, [e] | 0.814 | |
| | III-Me₂-Me | |
| V _{bur} , [%] | 60.2 | |
| (Cp _{cent} –M–Flu _{cent} bite angle [°]) | (118.99) | |
| NPA charge on M, [e] | 0.809 | |

| | | | |
|--|---|--|---|
| Steric maps |  |  |  |
| | III-PhH-Me/ III-PhH-Me-Hf | IV-PhH-Me | V-PhH-Me |
| V_{bur} , [%] | 59.7 / 60.2 | 60.1 | 63.5 |
| (C_{pcent} -M- Flu_{cent} bite angle [°]) | (117.91 / 118.72) | (118.12) | (118.69) |
| NPA charge on M, [e] | 0.836 / 0.996 | 0.835 | 0.870 |
| | | IV-Ph₂-Me | |
| V_{bur} , [%] | | 62.5 | |
| (C_{pcent} -M- Flu_{cent} bite angle [°]) | | (118.30) | |
| NPA charge on M, [e] | | 0.838 | |
| | | Si-IV-Ph₂-Me | |
| V_{bur} , [%] | | 63.2 | |
| (C_{pcent} -M- Flu_{cent} bite angle [°]) | | (128.66) | |
| NPA charge on M, [e] | | 0.796 | |

Scheme 7. Calculated data for a selected series of C_1 -symmetric {Cp/Flu} ansa-metallocene complexes: buried volumes (% V_{bur}) with sphere radius = 5.0 Å and C_{pcent} -M- Flu_{cent} bite angles [°] were computed for the geometries optimized at the B3PW91/LANL2DZ(f), SMD(toluene) level; NPA charges (e) computed at the same level of theory.

2.4. Polymerization Studies

2.4.1. Isospecific Polymerization of Propylene

Catalytic propylene polymerization experiments, carried out in a uniform manner for a series of {Cp/Flu}MCl₂ complexes activated with MAO (Scheme 8), revealed a remarkable influence of substitution patterns of metallocene precatalysts on the global polymerization performance and properties of polymers.^[21] Several trends were specifically drawn,^[22] evidencing the flexibility and limits of the polymerization processes with these catalytic systems:

a) In terms of productivity (as expressed in kg of PP-recovered per mmol of metallocene and per-hour), the most efficient ones were those based on **IV-Ph₂-Me** (50.7 kgPP·mmol⁻¹·h⁻¹), **V-PhH-Me** (34.5 kgPP·mmol⁻¹·h⁻¹) and **V-PhH-Et** (26.3 kgPP·mmol⁻¹·h⁻¹) that incorporate bulky substituents in the Flu ligands and Me or Et groups in the 5-Cp position. Yet, the most active systems within the {Cp/Flu} series remain significantly less productive than the benchmark **{SBI}-1** (135.75 kgPP·mmol⁻¹·h⁻¹) that belong to the family of C_2 -symmetric *rac*-bis(indenyl) systems. On the other hand, the poorest activity within the whole series was observed for the hafnium-based **III-PhH-Me-Hf** (0.26 kgPP·mmol⁻¹·h⁻¹), and also for **III-PhH-Ph** (1.36 kgPP·mmol⁻¹·h⁻¹) and **III-Me₂-Me** (1.71 kgPP·mmol⁻¹·h⁻¹) catalysts. The quite low polymerization activity of the hafnocene-based system is a result of the remarkable propensity of cationic species of the type $[(R_2C-(Flu)(Cp))HfMe]^+$ to form inactive "dormant" bimetallic species of the type $[(R_2C-(Flu)(Cp))Hf(\mu-Me)_2AlMe_2]^+$ through reaction with trimethylaluminum present in commercial MAO toluene solutions.^[23]

b) The presence of 5-Me or Et substituents in the Cp ligands have a critical effect for many catalysts, generally resulting in PPs with higher molecular weights. On the other hand, systems lacking these groups, namely **III-PhH-Ph** and **V-Ph₂**, produced polymers with significantly lower M_n values. An exception to this trend is **III-Ph₂** that has a similar substitution pattern to that of **V-Ph₂** but afforded high molecular weight polymers.

c) The stereoregularities of PPs produced with {Cp/Flu}-based catalysts, as expressed in terms of isotactic pentads [m]⁴, vary over quite a broad range depending on the substitution pattern. For example, the most stereoselective ([m]⁴ = 95.2–96.9 %) appeared to be metallocene systems incorporating a 5-Me Cp substituent, namely, **III-H₂-Me**, **III-Me₂-Me**, **III-PhH-Me**, and, quite unexpectedly, **III-Ph₂** having no such substituent. Logically, the PPs obtained with these systems also featured the highest melting transitions (T_m = 152–154 °C) within the whole series. The less stereoselective systems were **III-PhH-Ph** ([m]⁴ = 61.4 %) and **Si-IV-Ph₂-Me** ([m]⁴ = 31.9 %), also resulting in PPs with low melting transitions (T_m = 104 and 132 °C, respectively).

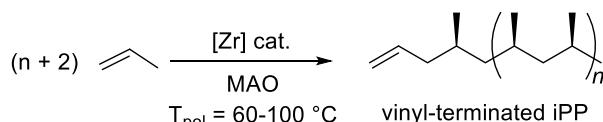
d) Incorporation of a Si-bridge had a negative effect on all the parameters (productivities, molecular weights, stereoregularities and T_m values), as evidenced upon comparing the results obtained with **Si-IV-Ph₂-Me** and its Ph₂C-bridged analogue **IV-Ph₂-Me**.

2.4.2. Synthesis of Vinyl End-Capped Isotactic-Enriched Oligopropylenes

Chain transfer reactions are inherent and inevitable elements of polymerization mechanisms that affect the molecular weight, chain-end functionalities and topology of polymers. The

predominant modes of chain termination in propylene polymerization are known to be monomolecular β -hydride elimination (or bimolecular β -hydride transfer to monomer) that give, after primary insertions, vinylidene-terminated chains, and chain-transfer to Me_3Al (always present in MAO) that provide saturated aliphatic terminal groups.^[24]

In the course of our studies, the capability of isoselective C_1 -symmetric zirconocenes **III-PhH-R** (R = Et, Ph), **IV-PhR-Me** (R = H, Ph) and **V-PhH-R** (R = Et, Ph) to produce oligo/polypropylenes bearing unsaturated chain-end groups via β -Me elimination was established (Scheme 9).^[17]

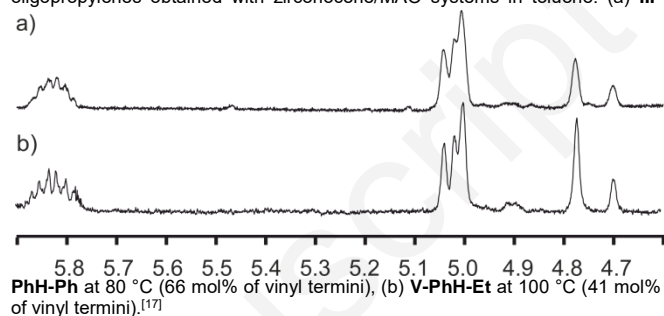


Scheme 9. Propylene oligo/polymerization leading to vinyl end-capped polymers via a β -methyl elimination mechanism.

The highest selectivity for generation of vinyl-terminated chains was observed with **III-PhH-Ph** which has a 5-Ph substituent on the Cp ring. Already at 60 °C, this precursor, activated with MAO, affords isotactic-enriched oligomers with 53–66 mol% of vinyl chain-ends (Figure 1). The content of vinyl chain-ends is not much affected by the polymerization temperature up to 100 °C, although, expectedly, lower molecular weight materials isolated as viscous oils were recovered in experiments conducted at 80 and 100 °C. These oligo/polymer materials featured also lower isotacticities ($[m]^4 = 4.6\text{--}19.9\%$) and, as a result, did show neither melting nor crystallization transitions. These materials can find applications as valuable comonomers (macromers) in copolymerization reactions with ethylene or α -olefins as well as for the production of long-chain branched

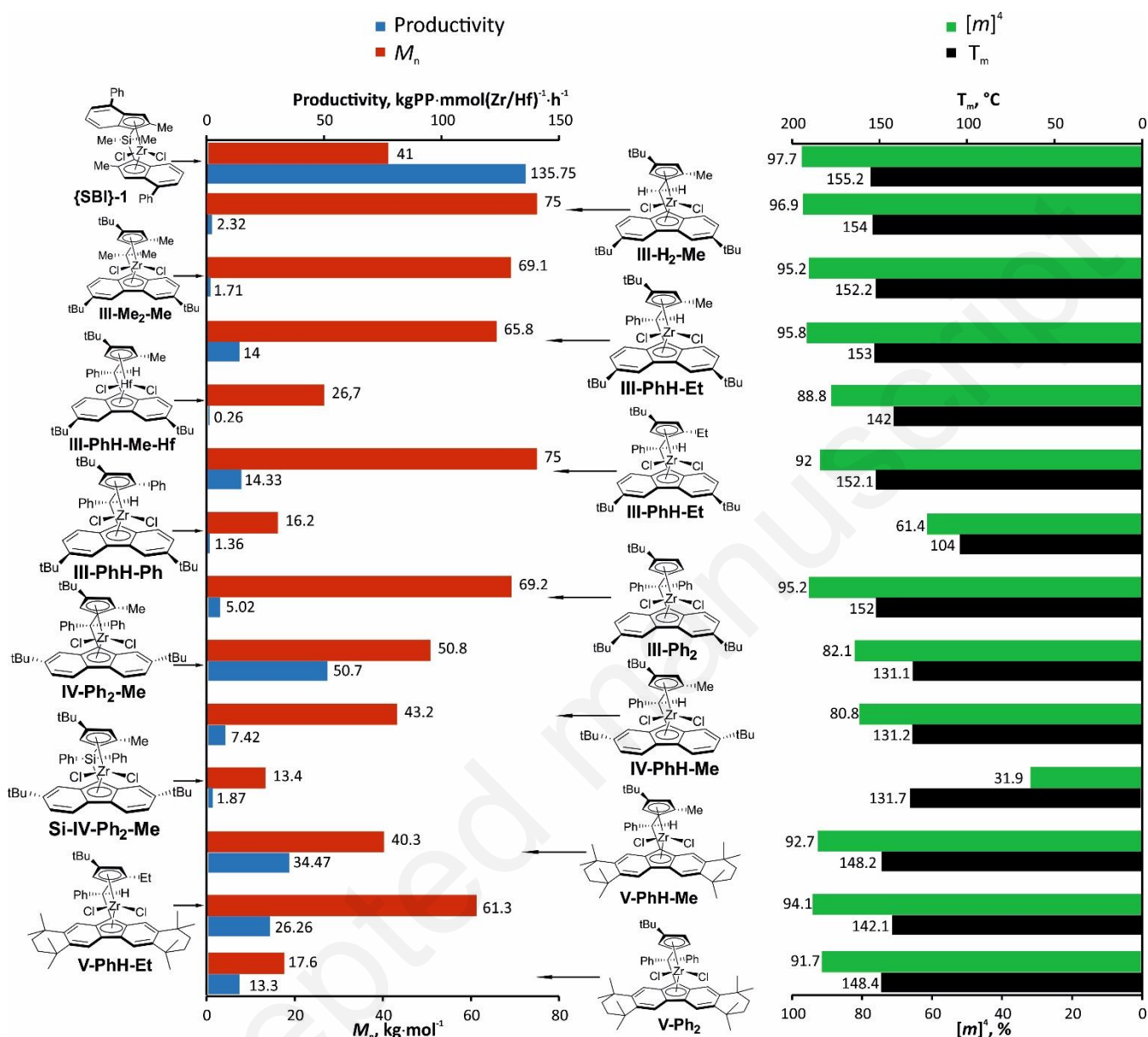
polymers with various topologies and unique properties.^[25] For example, commercial PP grades usually have relatively low melt strength and strain hardening behavior, which limits their use in applications such as thermoforming, foaming and blow molding. For the improvement of melt properties, such as melt strength and strain hardening behavior, introduction of long chain branches (LCB) by copolymerization with vinyl chain-end terminated iPP macromers appears to be the most efficient method.^[26]

Figure 1. ^1H NMR spectra (500 MHz, 100 °C, $\text{C}_2\text{D}_2\text{Cl}_4$) of vinyl end-capped oligopropylenes obtained with zirconocene/MAO systems in toluene: (a) **III-PhH-Ph** at 80 °C (66 mol% of vinyl termini), (b) **V-PhH-Et** at 100 °C (41 mol% of vinyl termini).^[17]

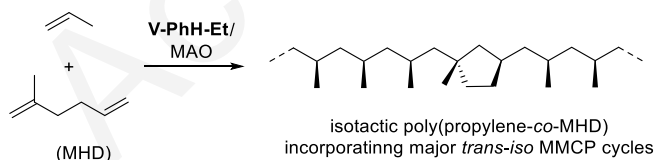


2.4.3. (Co)polymerization of Other Monomers

Targeting complex macromolecular structures that include in the polymer main-chain cyclic units interfaced by methylene groups,^[27] we became interested in copolymerization of short, non-conjugated diolefins such as 2-methyl-1,5-hexadiene (MHD) with propylene. The latter copolymerization was achieved with the isoselective metallocene precatalyst **V-PhH-Et** activated by MAO (Scheme 10).^[28]



Scheme 8. Selected propylene polymerization data obtained for {Cp/Flu}MCl₂/MAO systems and the reference {SBI}-1/MAO under homogeneous conditions (solvent: toluene, 60 °C, [MAO]/[M]₀ = 4,000–6,000, polymerization time: 30 min).^{[15],[16],[17]}



Scheme 10. Cyclopolymerization of MHD with propylene promoted by *ansa*-zirconocene catalyst **V-PhH-Et** (solvent: toluene, 60 °C, [MAO]/[Zr]₀ = 5000, polymerization time: 30 min).

ansa-zirconocene catalyst systems, which decreased by ca. 25–50%. As showcased with system **V-PhH-Et**/MAO, the amount of MHD incorporated in the copolymers appeared to be proportional to the concentration of monomer initially loaded (Figure 2). The cyclopolymerization of MHD affected the molecular features of the copolymer produced, and the resulting poly(propylene-co-MHD) copolymers featured molecular weights ($M_n = 33.3\text{--}44.8\text{ kg}\cdot\text{mol}^{-1}$) systematically lower than the corresponding homoPP samples.

The presence of MHD comonomer revealed a noticeable, slightly detrimental influence on the catalyst productivity of the

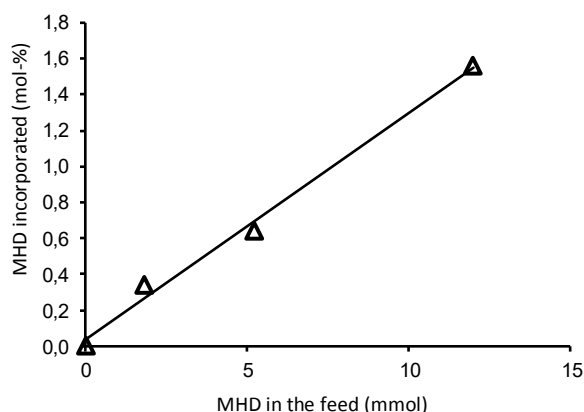


Figure 2. Plot of MHD incorporated in PP as a function of initial loading, with catalyst system **V-PhH-Et/MAO**. [Error! Bookmark not defined.]

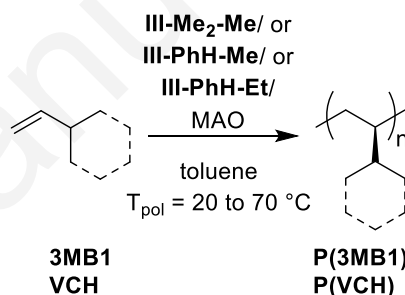
Detailed ^1H and ^{13}C NMR spectroscopic analyses of the copolymers evidenced complete cyclopolymerization of MHD with propylene, eventually providing isolated methylene-(1-methyl)-1,3-cyclopentane (MMCP) units (0.64–1.59 mol%) within the isotactic PP chains ($[m]^4 = 92.0\text{--}92.5\%$); no pendant vinylidene group was observed in any case. It was thus surmised that: (i) after insertion of a vinyl group of MHD, insertion of the MHD vinylidene group is favored over insertion of a propylene molecule; (ii) insertion of a propylene molecule after cycloinsertion of a MHD molecule is favored over possible β -Me elimination from a $[\text{Zr}]$ -MMCP reactive intermediate. Vinylidene insertion is also stereoselective, as corroborated by ^{13}C NMR analysis.

Also, the copolymerization of higher α -olefins comparable in size with MHD but having no additional polymerizable function, namely 8-trimethylsilyl-1-octene (8-TMSO) and 7-methyl-1,6-octadiene (1,6-MOD) proceeded with the **III-PhH-Et/MAO** system (which has similar reactivity and properties as **V-PhH-Et/MAO**). The drop of productivity and the amounts of 8-TMSO and 1,6-MOD incorporated were comparable to those observed for polymerization of MHD under similar conditions (*i.e.* ca. 0.3 mol%). These results were accounted for by the formation of a kind of “dormant” species issued from incorporation of the comonomers, which are poorly prone to propagation. Such sterically congested species could also exhibit a low propensity to undergo termination or chain transfer to aluminum reactions.

The latter phenomenon was also likely at the origin of the poor activity observed for several metallocene catalysts, namely **III-Me₂-Me**, **III-PhH-Et** and **III-PhH-Me**, in the homopolymerization of the sterically demanding 3-methylbut-1-ene (3MB1) and vinylcyclohexane (VCH) monomers (Scheme 11).^[29]

Modest productivities up to $15\text{ kg}\cdot\text{mol}^{-1}\cdot\text{h}^{-1}$ were obtained with 3MB1 (toluene, $20\text{ }^\circ\text{C}$), while higher productivities up to $75\text{ kg}\cdot\text{mol}^{-1}\cdot\text{h}^{-1}$ were obtained in the polymerization of VCH. Optimization of the polymerization conditions ($T_{\text{pol}} = 70\text{ }^\circ\text{C}$) led to a significant enhancement of the productivities of this catalyst system towards both 3MB1 and VCH, up to 390 and $760\text{ kg}\cdot\text{mol}^{-1}\cdot\text{h}^{-1}$, respectively. NMR spectroscopic analyses of a few soluble

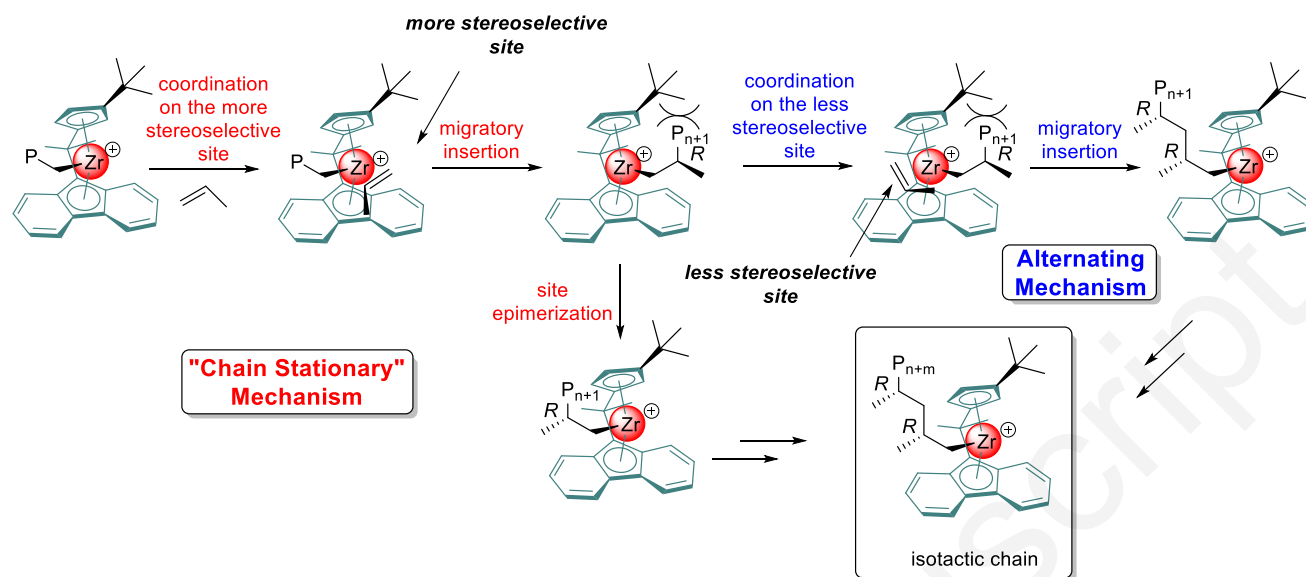
poly(3MB1)s and poly(VCH)s samples proved them to be isotactic, and a chain-end control was suggested to be the principal stereocontrol mechanism operative for polymerization of these two bulky monomers. The very poor solubility of the thus prepared poly(3MB1)s samples in regular solvents used for SEC (THF, CHCl_3 , trichlorobenzene), even at high temperature, prevented exhaustive analysis of molecular weights by this technique. An estimation of the M_n values was carried out by $^{13}\text{C}\{^1\text{H}\}$ NMR spectroscopy from integration of the chain-end and main-chain signals, demonstrating that the soluble part of P(3MB1) consists of oligomers with DP_n in the range 6–30. In the polymerization of VCH with **III-PhH-Et/MAO**, rising the polymerization temperature from 20 to $70\text{ }^\circ\text{C}$ resulted in poly(VCH) polymers with molecular weights one order of magnitude lower ($M_n = 61.2$ vs. $4.8\text{ kg}\cdot\text{mol}^{-1}\cdot\text{h}^{-1}$), as anticipated from enhanced β -H elimination and transfer processes at higher temperatures. All attempts to study the thermal properties of the poly(3MB1) and poly(VCH) polymers by DSC failed due to decomposition of samples at high temperatures, even under inert atmosphere.



Scheme 11. P(3MB1) and P(VCH) homopolymers obtained with **III-Me₂-Me/**, **III-PhH-Et/** and **III-PhH-Me/MAO**.

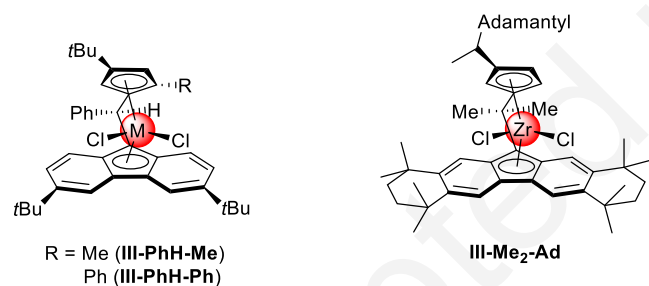
2.4.4. Origins of Stereoselectivity in Polymerization with C_1 -Symmetric {Cp/Flu}-ansa-Metallocene Catalysts

Enantiomeric site control (ESC) via ubiquitous chain migratory insertion has been corroborated as the operative mechanism for C_2 -symmetric {SBI}-type metallocene catalysts.^[30] In their pioneering contributions, Razavi *et al.*^{[7b,c],[31]} have suggested that a “chain stationary” insertion (also referred to as “site epimerization”) mechanism (Scheme 12), involving monomer insertion only on the more crowded/stereoselective site, followed by site epimerization (“backskip”), operates as the main mechanism of stereocontrol for C_1 -symmetric {Cp/Flu}-type metallocene catalysts. Marks *et al.*^[8f] have proposed an alternating mechanism leading to formation of isotactic sequences, which involves both a lesser (sterically open) and a more (sterically crowded) stereoselective sites of the metallocene for monomer insertion. Bercaw *et al.* have discussed a case in which both abovementioned mechanisms could be functioning simultaneously.^[9a,c]



Scheme 12. Proposed stereocontrol mechanisms with C_1 -symmetric metallocene catalysts.^[9a,c]

In our studies, aimed at rationalizing the mechanism of regio- and stereocontrol of the highly isoselective polymerization of propylene with complexes **III-PhH-Me**, **III-PhH-Ph** and **V-Me₂-Ad**^[9c] (Scheme 12), theoretical computations were carried out for the first, second and third propylene insertion steps.^[32]



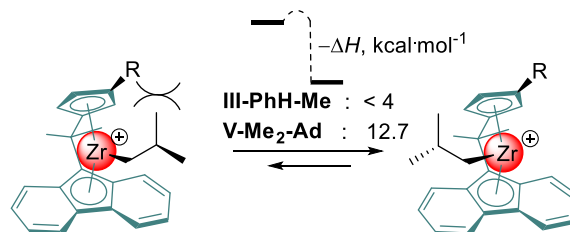
Scheme 13. Zirconocene precatalysts **III-PhH-R** ($R = \text{Me, Ph}$)^[17] and **V-Me₂-Ad**^[9c] used as models in DFT studies.

On the basis of the computational results obtained for systems **III-PhH-R** ($R = \text{Me, Ph}$) and **V-Me₂-Ad**, the following trends and conclusions were highlighted:

1) Regardless the actual monomer insertion step, primary (1,2-) coordination and insertion of propylene into $\text{Zr}-\text{C}(\text{alkyl})$ bond are systematically highly selective for all systems, which is evidenced from the corresponding lower activation barriers (typically by 3–11 $\text{kcal}\cdot\text{mol}^{-1}$) than those calculated for secondary (2,1-) insertions. This appears to be driven in part by steric considerations, and higher thermodynamic stability of the Zr -polymeryl products resulting from the 1,2-insertions.

2) The very first propylene insertion into $\text{Zr}-\text{Me}$ bond is *not* stereoselective; stereoselectivity control over monomer insertion

for the C_1 -symmetric systems comes out from the second insertion step, that is propylene insertion in the $\text{Zr}-\text{C}(\text{tBu})$ bond. Computational results also evidenced that, after the primary (*si*) insertion on the more stereoselective site (Scheme 12), the resulting sterically-congested product with the propagating polymer chain initially residing on the crowded site should rearrange via epimerization (Scheme 14) to a less sterically congested, more stable (by ca. 4 or 12.7 $\text{kcal}\cdot\text{mol}^{-1}$ for **III-PhH-Me** and **V-Me₂-Ad**, respectively) *anti* isomer. This sequence of insertion-epimerization steps leads to the formation of iPP by a chain “stationary” insertion mechanism.



Scheme 14. Epimerization (“backskip”) process for C_1 -symmetric $\{\text{Cp}/\text{Flu}\}$ metallocene catalysts.

3) For **III-PhH-Ph**, the computed data were also in complete agreement with the epimerization mechanism; however, the smaller energy difference between the barriers of misinsertion and stereoselective primary (*si*) insertion ($\Delta\Delta H^\ddagger = 3.1 \text{ kcal}\cdot\text{mol}^{-1}$) suggested a lesser stereoselectivity of that system. Also, the higher propylene (*pr-si*) insertion barrier calculated for **III-PhH-Ph** ($\Delta\Delta H^\ddagger = 1.5 \text{ kcal}\cdot\text{mol}^{-1}$) accounted for the observed lower polymerization activity as compared to many other systems (Scheme 8).

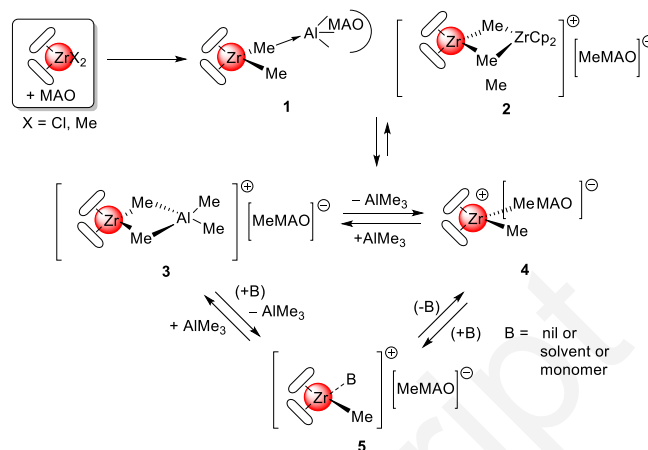
4) The validity of the “chain stationary” insertion mechanism (i.e., site epimerization by “backskip”) for isoselective C_1 -symmetric {Cp/Flu}-type metallocenes used in our studies was demonstrated. At the same time, the aforementioned alternative, yet less stereoselective alternating mechanism of stereocontrol can be operational. The steric bulkiness imposed by the 3-Cp substituent (i.e., 2-methyl-2-adamantyl in **V-Me₂-Ad** vs *t*Bu in **III-PhH-Me**) was shown to be beneficial for the suppression of this alternative mechanism. On the other hand, introduction of a bulkier group (Ph vs Me) into the 5-Cp position facilitated the alternating mechanism, eventually affording a less stereoselective catalyst.

5) The thermochemical data obtained through the computational study were used to predict microstructures of PPs using three-parameter statistical models for the {Cp/Flu}-type metallocene systems. The calculated *meso/rac* pentad distributions were found in good agreement with those determined experimentally for iPP samples obtained at different polymerization temperatures.

3. Studies on the Nature and Quantification of Active Sites in Metallocene Polymerization Catalysis

3.1. Structure and Solution Dynamics of Metallocenium Ionic Complexes

It is well known that the efficiency and stability of a catalytic system crucially depends on precatalyst activation protocols for generating ionic species responsible for polymerization.^{[33],[34]} Combinations of group 4 metal precursors Cp_2MX_2 (L = ligand, X = Me, Cl) with methylaluminoxane (MAO) give rise to complex reaction mixtures, generally consisting of diamagnetic M(IV) products of the type **1–5** (Scheme 15) with different electropositivity of the metal center and cation-anion separation with different extents, i.e., inner-sphere (ISIP) vs outer-sphere (OSIP) ion-pairs. In some cases, concomitant formation of paramagnetic M(III) species during activation of some dichloro-metallocenes (M = Ti, Zr) with MAO (or “AlMe₃-depleted” MMAO) has been detected by ESR spectroscopy.^[35] The speciation from these reaction mixtures depends, in principle, on such parameters as nature of metal precatalyst, [MAO]/[M] ratio, composition of MAO, nature of solvent, duration of activation (“aging”), etc. Among the resulting species formed, ISIP species **4** are believed to be the immediate precursors of the “true” polymerization catalyst $[Cp_2ZrMe(B)]^+$, the OSIP species **5**, which forms through a reorganization or expulsion of the [Me-MAO]⁻ anion from the inner to the outer coordination sphere. On the other hand, the OSIP AlMe₃-adduct **3** is the dominant component of this milieu and is often considered as a “dormant” species,^[36] acting as the reservoir of both **4** and **5**.

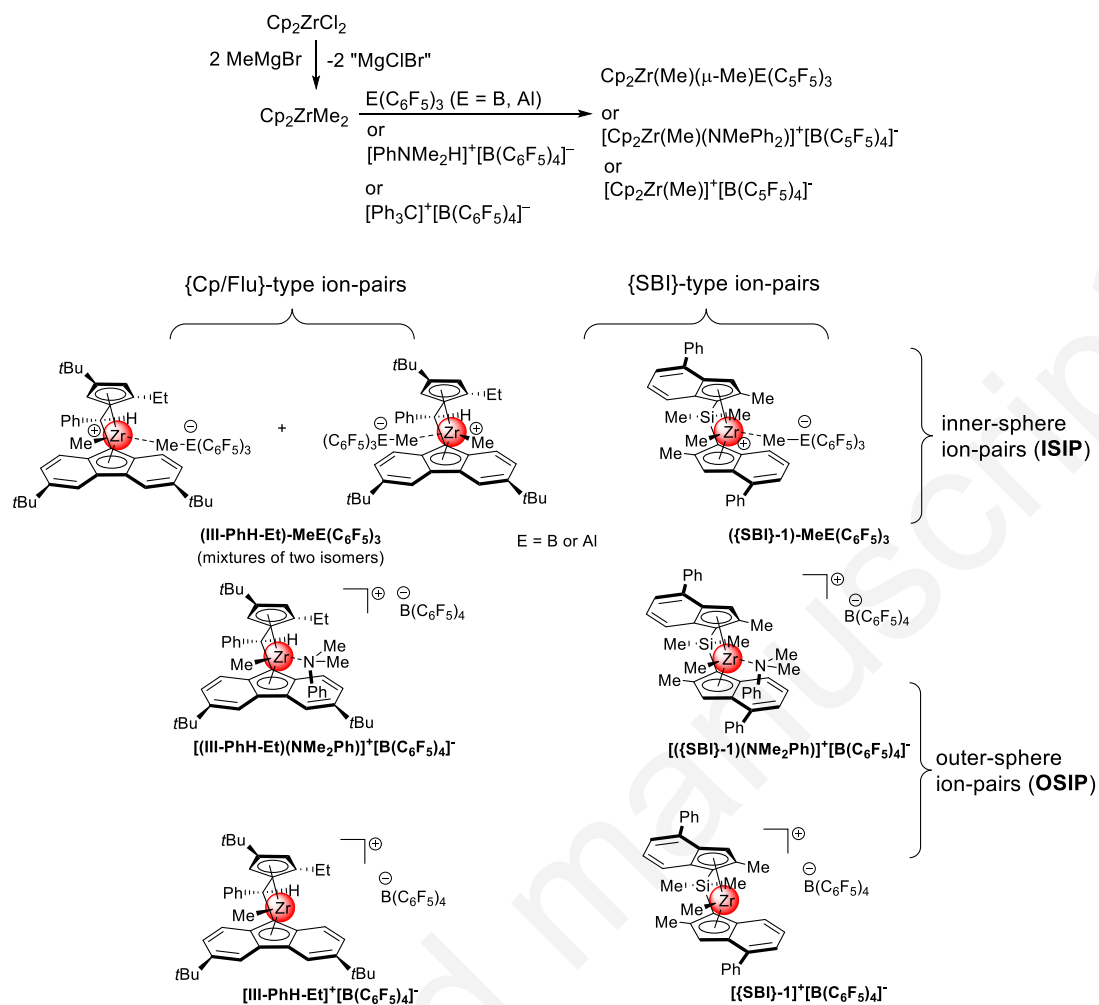


Scheme 15. Putative Zr(IV) intermediates and products (**1–5**) that form upon activation of zirconocenes with MAO.

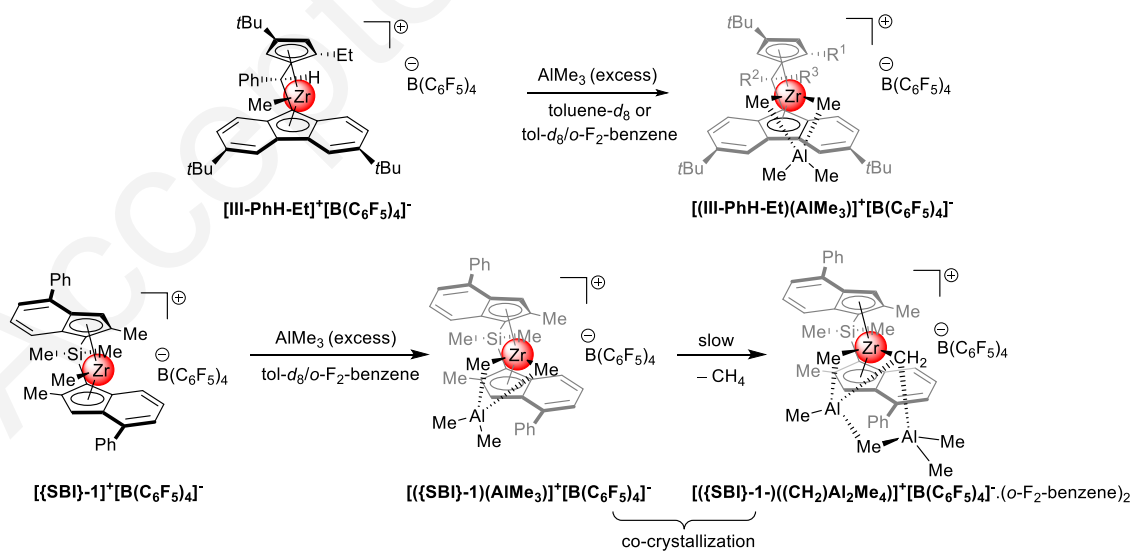
In our studies, we investigated the role of activation conditions of metallocene catalysts, as well as ion-pairing effects and anion dynamics in the metal coordination sphere for developing more efficient (in terms of productivity, stability, stereoselectivity and PP properties) catalytic combinations and more effective activation protocols. In particular, we aimed at understanding the so-far misunderstood origin of the much different productivity and possible different behavior between isoselective {SBI}- and {Cp/Flu}-type propylene polymerization precatalysts (Scheme 8). As a matter of fact, the former catalysts (e.g. **{SBI}-1**) are typically one order of magnitude more productive than the latter systems, both under homogeneous, but also under heterogeneous (supported, slurry) conditions, still providing the same level of stereocontrol.

For these studies, a series of discrete stable metallocenium ion-pairs, presumed to be structurally similar to those derived from MAO, was obtained by treatment of the parent neutral dialkyl metallocenes with appropriate molecular activators (Scheme 16), including highly electrophilic boranes and alanes, $E(C_6F_5)_3$ (E = B, Al), and borate salts of the type $[R]^+[B(C_6F_5)_4]^-$ (R = Ph₃C, HNMe₂Ph).^{[37],[38]} The solution structures of the ion-pairs were studied by multinuclear (¹H, ¹¹B, ¹³C and ¹⁹F) and 2D (HETCORR, NOESY, HOESY and EXSY) NMR spectroscopy in toluene-*d*₆ (or toluene-*d*₆/*o*-difluorobenzene mixtures).

The DOSY PGSE-derived hydrodynamic radii for the inner-sphere ion-pairs (ISIP) **(III-PhH-Et)-MeE(C₆F₅)₃** and **({SBI}-1)-MeE(C₆F₅)₃** incorporating $MeB(C_6F_5)_3^-$ or $MeAl(C_6F_5)_3^-$ anions measured at different concentrations, and the aggregation number values calculated therefrom, were all consistent with monomeric associated structures in solution. The molecular solid-state structures of the zwitterionic **(III-PhH-Et)-MeB(C₆F₅)₃**, **({SBI}-1)-MeB(C₆F₅)₃** and **({SBI}-1)-MeAl(C₆F₅)₃** were determined by X-ray crystallography and found consistent with the solution structures, in which the $MeE(C_6F_5)_3^-$ anions are bound to the metal center (in case of **(III-PhH-Et)-MeB(C₆F₅)₃**, via the open face of the metallocenium cation).



35 **Scheme 16.** Generation of ion-pairs (ISIP and OSIP) by reactions of dimethyl-zirconocenes with one equiv of E(C₆F₅)₃ (E = B, Al), [PhNMe₂H]⁺[B(C₆F₅)₄]⁻ and
36 [Ph₃C]⁺[B(C₆F₅)₄]⁻.^[37]



57 **Scheme 17.** Formation of AlMe₃-adducts [[(III-PhH-Et)(AlMe₃)]⁺[B(C₆F₅)₄]⁻ and [[(SBI)-1](AlMe₃)]⁺[B(C₆F₅)₄]⁻ / [[(SBI)-1)((CH₂)Al₂Me₄)]⁺[B(C₆F₅)₄]⁻ by reactions of
58 complexes [[(III-PhH-Et)]⁺[B(C₆F₅)₄]⁻ and [[(SBI)-1]]⁺[B(C₆F₅)₄]⁻ with excess AlMe₃, respectively.^[37]

The PGSE data obtained for the outer-sphere ion-pairs (OSIP) $[(\text{III-PhH-Et})(\text{NMe}_2\text{Ph})]^+[\text{B}(\text{C}_6\text{F}_5)_4]^-$ and $[(\{\text{SBI}-1\})(\text{NMe}_2\text{Ph})]^+[\text{B}(\text{C}_6\text{F}_5)_4]^-$ in toluene-*d*₆/*o*-F₂-benzene mixtures suggested that both species are higher aggregates.

Heterobimetallic ion-pairs of the type $[\{\text{LX}\}_2\text{M}(\mu\text{-R})\text{AlR}_2]^+[\text{A}]^-$ (where $\{\text{LX}\}_2\text{M}$ = group 4 metallocene-type core; R = alkyl; $[\text{A}]^-$ = counteranion such as $[\text{MeMAO}]^-$, $[\text{B}(\text{C}_6\text{F}_5)_4]^-$, etc) are recognized as “dormant” species and precursors of chain-transfer in polymerization. In order to mimic the formation of heterobimetallic species, the reactivity of ion-pairs towards AlMe_3 was investigated. Treatment with excess AlMe_3 of complexes $[(\text{III-PhH-Et})]^+[\text{B}(\text{C}_6\text{F}_5)_4]^-$ and $[(\{\text{SBI}-1\})]^+[\text{B}(\text{C}_6\text{F}_5)_4]^-$, generated in situ from the parent dimethyl precursors and 1 equiv of $[\text{Ph}_3\text{C}]^+[\text{B}(\text{C}_6\text{F}_5)_4]^-$ in a toluene-*d*₆/*o*-F₂-benzene mixture at room temperature, resulted in the immediate and clean formation of the deep-blue and deep-red cationic heterobimetallic adducts $[(\text{III-PhH-Et})(\text{AlMe}_3)]^+[\text{B}(\text{C}_6\text{F}_5)_4]^-$ and $[(\{\text{SBI}-1\})(\text{AlMe}_3)]^+[\text{B}(\text{C}_6\text{F}_5)_4]^-$, respectively (Scheme 17).

Solution NMR spectroscopic data, acquired immediately on freshly prepared samples of $[(\text{III-PhH-Et})(\text{AlMe}_3)]^+[\text{B}(\text{C}_6\text{F}_5)_4]^-$ and $[(\{\text{SBI}-1\})(\text{AlMe}_3)]^+[\text{B}(\text{C}_6\text{F}_5)_4]^-$, were indicative of C₁ and an average C₂ symmetry, respectively. The DOSY NMR spectroscopy-derived translation diffusion coefficients, hydrodynamic radii and the aggregation number values calculated therefrom were all consistent with the monomeric nature of these ionic complexes in solution.

While attempts to grow crystals of $[(\text{III-PhH-Et})(\text{AlMe}_3)]^+[\text{B}(\text{C}_6\text{F}_5)_4]^-$ failed, red single crystals of its analogue $[(\{\text{SBI}-1\})(\text{AlMe}_3)]^+[\text{B}(\text{C}_6\text{F}_5)_4]^-$ were readily obtained. The X-ray diffraction studies revealed that two different species co-crystallize together as 1:1 mixed crystals of the expected heterobimetallic complex $[(\{\text{SBI}-1\})(\text{AlMe}_3)]^+[\text{B}(\text{C}_6\text{F}_5)_4]^-$ and the monocationic heterotrimetallic methylidene species $[(\{\text{SBI}-1\})(\mu\text{-CH}_2)\text{Al}_2\text{Me}_4]^+[\text{B}(\text{C}_6\text{F}_5)_4]^-$ (*o*-F₂-benzene)₂ (Figure 3). The latter complex was surmised to be the product of a C–H activation process involving one of the two Zr(μ -Me)₂Al bridging-methyl groups in $[(\{\text{SBI}-1\})(\text{AlMe}_3)]^+[\text{B}(\text{C}_6\text{F}_5)_4]^-$ and an additional AlMe_3 molecule, implying concomitant release of a molecule of CH₄.

To get a better insight in the dynamic behavior of the metallocenium ion-pairs $(\text{III-PhH-Et})\text{-MeE}(\text{C}_6\text{F}_5)_3$ and $(\{\text{SBI}-1\})\text{-MeE}(\text{C}_6\text{F}_5)_3$ (E = B, Al), the EXSY component of the ¹H–¹H NOESY spectra was studied in the temperature range 5–45 °C. Two mechanisms of reorganization/exchange (site epimerization) were identified: lateral side-anion exchange (AE) of the entire $\text{MeB}(\text{C}_6\text{F}_5)_3^-$ anion, and neutral $\text{B}(\text{C}_6\text{F}_5)_3$ coactivator exchange (CE) between the Zr–Me groups. For $(\text{III-PhH-Et})\text{-MeB}(\text{C}_6\text{F}_5)_3$, the exchange involved predominantly a process of ion-pair reorganization *via* lateral side exchange of the $\text{MeB}(\text{C}_6\text{F}_5)_3^-$ anion between the two isomeric forms (Scheme 18; Table 1). The alane-based ion-pair $(\text{III-PhH-Et})\text{-MeAl}(\text{C}_6\text{F}_5)_3$ did not exhibit any visible exchange in toluene-*d*₆, even at elevated temperatures (> 60 °C) at which significant decomposition started.

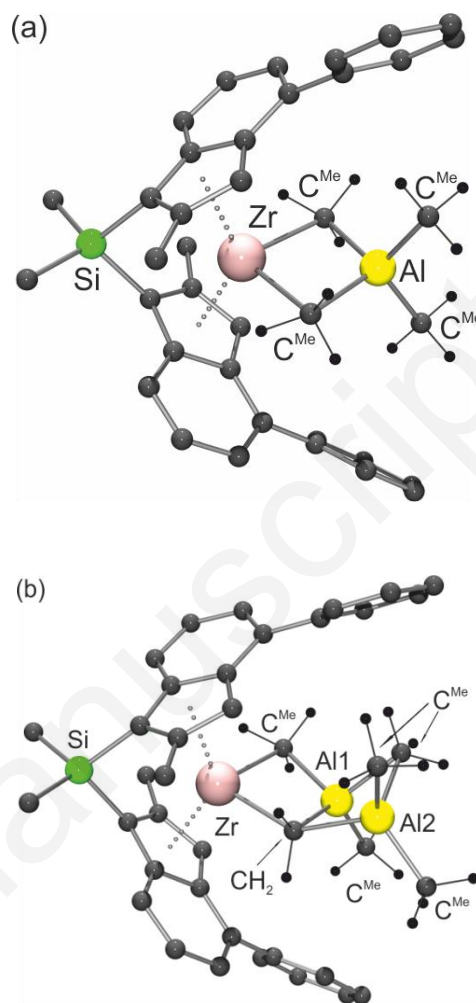
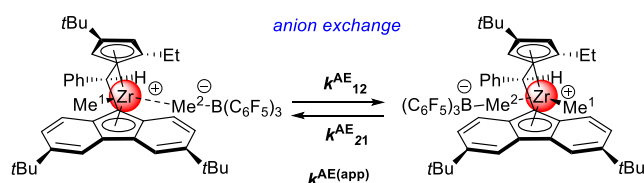
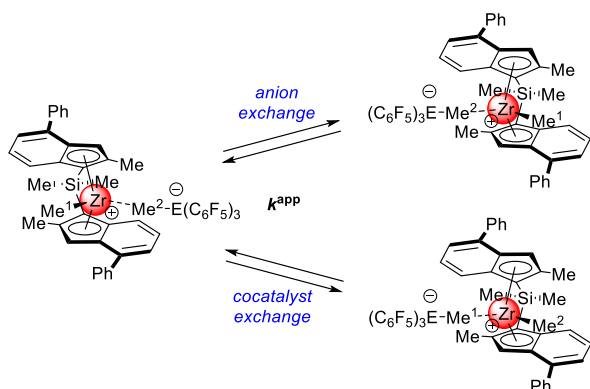


Figure 3. Molecular structures of: (a) $[\text{rac}\{-\text{Me}_2\text{Si}\{-2\text{-Me-4-Ph-Ind}\}_2\}\text{Zr}(\mu\text{-Me})_2\text{AlMe}_2]^+ [(\{\text{SBI}-1\})(\text{AlMe}_3)]^+$; (b) $[\text{rac}\{-\text{Me}_2\text{Si}\{-2\text{-Me-4-Ph-Ind}\}_2\}\text{Zr}(\mu\text{-CH}_2)(\mu\text{-Me})\text{AlMe}(\mu\text{-Me})(\text{AlMe}_2)_2]^+ [(\{\text{SBI}-1\})(\mu\text{-CH}_2)\text{Al}_2\text{Me}_4)]^+$ (all hydrogen atoms, $[\text{B}(\text{C}_6\text{F}_5)_4]^-$ anions and molecules of *o*-F₂-benzene are omitted for clarity).^[37]



Scheme 18. Predominant site-epimerization processes observed for the $\{\text{Cp}/\text{Flu}\}$ ISIP $(\text{III-PhH-Et})\text{-MeB}(\text{C}_6\text{F}_5)_3$.^[37]

In contrast with the $\{\text{Cp}/\text{Flu}\}$ systems, both types of exchange processes were found operational for the $\{\text{SBI}\}$ -type ion-pair $(\{\text{SBI}-1\})\text{-MeB}(\text{C}_6\text{F}_5)_3$ (Scheme 19). For the alane-based analogue $(\{\text{SBI}-1\})\text{-MeAl}(\text{C}_6\text{F}_5)_3$, the exchange processes were two orders of magnitude slower than those observed with the borane congener.



Scheme 19. Site-epimerization processes observed for the {SBI} ISIP ($\{SBI\}\text{-}1\text{-}MeE(C_6F_5)_3$ ($E = B, Al$)).^[37]

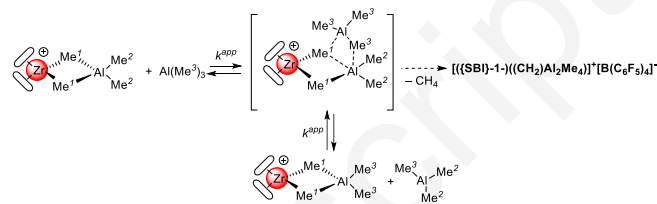
Table 1. Selected EXSY-derived apparent rate constants and activation parameters for exchange processes in ionic complexes.^{[a], [37]} ^[a] Determined by $^1H\text{-}^1H$ EXSY NMR spectroscopy in toluene- d_6 / o - F_2 -benzene (8:2 v/v) solutions, $[Zr]_0 = 10\text{--}28$ mM. ^[b] Rate constants are given at 298 K. ^[c] $[Al]_0 = 55.0\text{--}82.0$ mM.

| Complex | k^{app} [b] [$M^{-1}\cdot s^{-1}$] | ΔH^\ddagger [$kcal\cdot mol^{-1}$] | ΔS^\ddagger [$cal\cdot mol^{-1}\cdot K^{-1}$] | ΔG^\ddagger_{298} [$kcal\cdot mol^{-1}$] |
|--|---|---|--|---|
| $\{III\text{-}PhH\text{-}Et\}\text{-}MeE(C_6F_5)_3$ | 104(21) | 17.6(1) | 2(1) | 17.1(1) |
| $\{SBI\}\text{-}1\text{-}MeB(C_6F_5)_3$ | 246(7) | 17.6(1) | 5(1) | 16.2(1) |
| $\{SBI\}\text{-}1\text{-}MeAl(C_6F_5)_3$ | 151(7) | 8.1(1) | -31(1) | 17.3(1) |
| $\{III\text{-}PhH\text{-}Et\}(AlMe_3)_2^+ [B(C_6F_5)_4]^-$ [c] | 3.2(3) | 8.5(2) | -28(2) | 16.70(8) |
| $\{SBI\}\text{-}1\text{-}1(AlMe_3)_2^+ [B(C_6F_5)_4]^-$ [c] | 447(127) | 14.95(1) | 3.5(1) | 13.93(4) |

The dynamic behavior of freshly prepared samples of $AlMe_3$ -adducts $\{III\text{-}PhH\text{-}Et\}(AlMe_3)_2^+ [B(C_6F_5)_4]^-$ and $\{SBI\}\text{-}1\text{-}1(AlMe_3)_2^+ [B(C_6F_5)_4]^-$ was investigated by $^1H\text{-}^1H$ EXSY spectroscopy at variable temperatures in toluene- d_6 / o - F_2 -benzene solutions. The EXSY NMR spectra recorded for these two systems with $AlMe_3$ revealed rapid exchange between the methyl groups of “free” $AlMe_3$ (Me^3) and those of the terminal $Al(Me^2)_2$ moieties (Scheme 20). The fact that the rates of this exchange process for both systems $\{III\text{-}PhH\text{-}Et\}(AlMe_3)_2^+ [B(C_6F_5)_4]^-$ and $\{SBI\}\text{-}1\text{-}1(AlMe_3)_2^+ [B(C_6F_5)_4]^-$ were found at least one order of magnitude higher than those for the exchange between “free” $AlMe_3$ and the bridging-methyl $Zr(\mu\text{-}Me^1)_2Al$ groups (Table 1) discarded a dissociative mechanism involving reformation of the “naked” ion-pairs $\{III\text{-}PhH\text{-}Et\}^+ [B(C_6F_5)_4]^-$ and $\{SBI\}\text{-}1\text{-}1^+ [B(C_6F_5)_4]^-$ and “free” $AlMe_3$. Moreover, the fact that the initially observed magnetization exchange constants k^{obs}_1 and k^{obs}_{-1} for both systems ($k^{app} = k^{obs}_1/[AlMe_3] = k^{obs}_{-1}/[Zr]$) depended on the $AlMe_3$ concentration (provided the monomer/dimer equilibrium for $AlMe_3$ is very rapidly maintained on the time scale of the methyl group exchange) suggested that the rate-determining step is the formation of heterotrimetallic intermediates (i.e., $\{III\text{-}PhH\text{-}Et\}^+\cdot(AlMe_3)_2$ and $\{SBI\}\text{-}1\text{-}1^+\cdot(AlMe_3)_2$) through reversible binding of another molecule of $AlMe_3$ with $\{III\text{-}PhH\text{-}Et\}(AlMe_3)_2^+ [B(C_6F_5)_4]^-$ and $\{SBI\}\text{-}1\text{-}1(AlMe_3)_2^+ [B(C_6F_5)_4]^-$ (Scheme 20), respectively.

The two other exchange processes, namely the bridging- $Me^1/Al(Me^3)_3$ exchange and the bridging- Me^1 /terminal- Me^2 groups exchange, were also observed for both ion-pairs; they proceeded, however, with much lower rates than those observed for the predominant terminal $Me^2/Al(Me^3)_3$ groups exchange.

Exclusively for the {SBI}-type putative heterotrimetallic intermediate $\{SBI\}\text{-}1\text{-}1^+\cdot(AlMe_3)_2$, the slow decomposition process is operational, releasing CH_4 and the $\{SBI\}\text{-}1\text{-}1(\mu\text{-}CH_2)Al_2Me_4]^+ [B(C_6F_5)_4]^-$ product.



Scheme 20. Terminal- $Me/AlMe_3$ groups exchange process observed in metallocene $AlMe_3$ -adducts $\{III\text{-}PhH\text{-}Et\}(AlMe_3)_2^+ [B(C_6F_5)_4]^-$ and $\{SBI\}\text{-}1\text{-}1(AlMe_3)_2^+ [B(C_6F_5)_4]^-$.^[37]

Overall, the various data obtained for these ion-pairs (Table 1) allowed us to draw the following conclusions:

- the different exchange processes established for ion-pairs are systematically faster in case of the {SBI}-based systems as compared to those observed for the {Cp/Flu}-based congeners. These exchange phenomena patterns may be paralleled with the much higher catalytic productivities generally observed for {SBI}-based metallocene systems in olefin polymerization processes as compared to those of their {Cp/Flu}-based congeners. We surmised that the high rates of reorganization of different {SBI}-type species implying rearrangement of the counter-anion and/or $AlMe_3$ ligands in the coordination sphere of zirconium may induce larger amounts of active initiating species.
- the experimentally determined (UV/Vis spectroscopy, Figure 4a) absorption bands λ_{max} and the corresponding TD-DFT calculated LMCT transitions (Figure 4b) were well in line with the higher electrophilicity of the {Cp-Flu} species as compared to the related {SBI}-congeners.

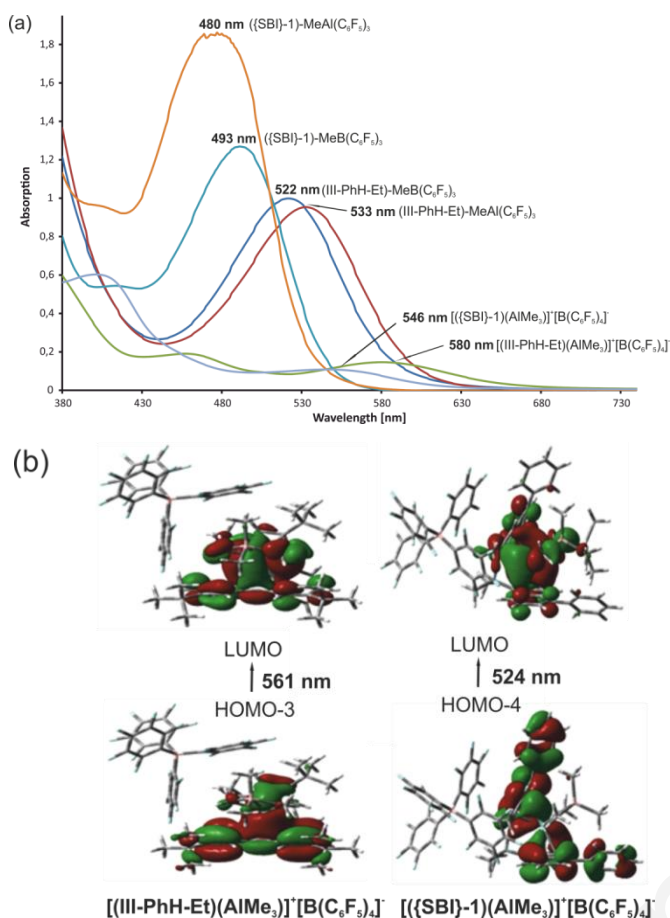


Figure 4. (a) Selected UV/Vis spectroscopic data for complexes (III-PhH-Et)-MeE(C₆F₅)₃ and ((SBI)-1)-MeE(C₆F₅)₃ (E = B, Al), [(III-PhH-Et)(AlMe₃)]⁺[B(C₆F₅)₄]⁻ and [(SBI)-1)(AlMe₃)]⁺[B(C₆F₅)₄]⁻ (0.5–0.6 mM in toluene); (b) Relevant frontier molecular orbitals of the optimized complexes [(III-PhH-Et)(AlMe₃)]⁺[B(C₆F₅)₄]⁻ and [(SBI)-1)(AlMe₃)]⁺[B(C₆F₅)₄]⁻ corresponding to maximal absorption bands λ_{\max} in UV-Visible spectra.^[37a]

3.2. Kinetic Studies and Activation Efficiency

In order to evaluate the ability of systems based on {SBI}- and {Cp/Flu}-type zirconocene complexes in generating the active form(s) of catalyst, kinetic investigations were conducted via determination of the propagation rate constants, the apparent k_p^0 and the specific k_p , and the fraction of active species formed χ^* .^{[39],[40]} For these studies, a kinetic method developed by Bochmann *et al.*^[41] was used, which is based on determination of the time dependence of monomer conversion (Figure 5) and M_n of polymer in polymerization of 1-hexene. Also, the influence of aging conditions on activity was investigated (Table 2).

For the {SBI}-1/MAO system, no significant influence of the aging conditions on activity was observed; the propagation rate constants k_p^0 calculated at 2 and 60 min of aging were very close. Also, the amount of active sites as well as molecular weight characteristics remained constant throughout this time period. Interestingly, for (III-Me₂-Me) and (III-Ph-Et), the apparent propagation rate constants ($k_p^0 = 0.52(6)$ and $0.47(5)$ L·mol⁻¹·s⁻¹, respectively) calculated at the early stages of polymerization are comparable or very close to those obtained for the {SBI}-based

counterpart. However, the specific propagation rate constants ($k_p = 8.2(7)$ and $52(8)$ L·mol⁻¹·s⁻¹, respectively) were found to be one order of magnitude higher, which returned quite poor activation efficiency for both systems ($\chi^* = 0.06(2)$ and $0.009(2)$, respectively). Yet, the overall activities of these systems rapidly decreased over time: no further monomer conversion was observed after ca. 0.5 and 8 h, respectively. For (III-Me₂-Me), when both aging and polymerization were performed at 60 °C, 1-hexene was fully consumed and concomitant formation of 2-hexene (by 1-hexene isomerization) was evidenced by ¹H NMR spectroscopy. This side reaction also occurred at 30 °C but to a lesser extent (ca. 10% of 2-hexene formed after 6 h).

For (III-PhH-Et), the same isomerization reaction took place at 60 °C giving only 10% of 2-hexene after 6 h, while no isomerization was observed for (IV-Ph₂-Me). The latter (IV-Ph₂-Me)/MAO system followed perfect first-order kinetics under these conditions, leading to full conversion of 1-hexene after 6 h, and yielded the highest k_p^0 and k_p values within the whole series (16(5) and 131(42) L·mol⁻¹·s⁻¹, respectively). Very similar results (in terms of kinetics) were obtained with a close analogue, complex (IV-PhH-Me) incorporating only a single phenyl group in the PhHC-bridge.

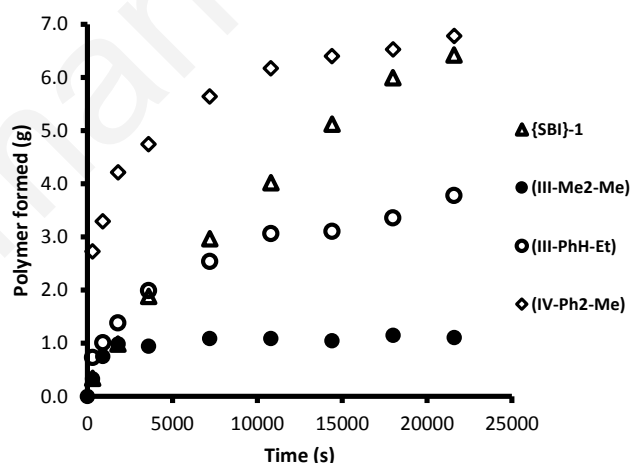


Figure 5. Overview of kinetic monitoring experiments of 1-hexene polymerization with different zirconocene/MAO systems (Table 2); reaction conditions: $T_{\text{aging}} = T_{\text{polym}} = 30$ °C; $[Zr]_{\text{tot}} = 0.20$ mM; $[1\text{-hexene}]_0 = 1.6$ M in toluene (6.73 g, 80.5 mmol); $[MAO]/[Zr]_{\text{tot}} = 1000$.^[40]

Table 2. Values of k_p^0 , k_p (in L·mol⁻¹·s⁻¹), χ^* , M_n (in kDa) and \mathcal{D}_m for different zirconocene/MAO systems.^[40]

| Precatalyst | Aging time [min] | k_p^0 | k_p | $\chi^* = k_p^0/k_p$ | M_n | \mathcal{D}_m |
|---------------------------|------------------|---------|--------|----------------------|-----------|-----------------|
| {SBI}-1 | 60 | 0.30(3) | 7(2) | 0.33(4) | 43.6/44.9 | 1.65/1.61 |
| | 2 | 0.49(5) | 4(2) | 0.37(7) | 50.7 | 1.60 |
| (III-Me ₂ -Me) | 60 | 0.52(9) | 8.2(7) | 0.06(2) | 37.9 | 1.25 |
| | 10 | 0.30(7) | 8(1) | 0.04(1) | 41.9 | 1.16 |
| (III-PhH-Et) | 2 | 1.3(2) | 2.4(4) | 0.5(2) | 32.1/30.3 | 1.19/1.20 |
| | 60 | 0.52(9) | 8.2(7) | 0.06(2) | 37.9 | 1.25 |

| | | | | | | |
|-------------------------------|----|---------|---------|----------|-------------|-----------|
| | 60 | 0.47(5) | 52(8) | 0.009(2) | 87.0/89.1 | 1.30/1.33 |
| (III-PhH-Et) | 10 | 1.6(8) | 27(4) | 0.06(4) | 87.1/88.8 | 1.29/1.32 |
| | 2 | 1.4(3) | 12(2) | 0.12(2) | 76.7/75.2 | 1.29/1.42 |
| | 60 | 16(5) | 131(42) | 0.12(6) | 115.5 | 1.43 |
| (IV-Ph₂-Me) | 10 | 10(5) | 220(70) | 0.05(2) | 109.1/110.2 | 1.45/1.45 |
| | 2 | 8.8(7) | 61(8) | 0.14(4) | 114.3/115.0 | 1.33/1.34 |

Reaction conditions, unless otherwise stated: $[Zr]_{tot} = 0.20$ mM; $[1\text{-hexene}]_0 = 1.6$ M in toluene; $[MAO]/[Zr]_{tot} = 1000$.

Remarkably, upon decreasing the aging time from 60 to 10 and 2 min, a significant decrease of activity (as reflected by the k_p values) was observed for the three {Cp/Flu}-type catalysts (Table 2); the trend was more pronounced for the **(III-Me₂-Me)**/MAO system. For the three systems, the fraction of active sites determined at shorter aging time was found systematically higher, thus suggesting degradation of active sites to a significant extent (especially for **(III-Me₂-Me)**) over time during the aging period in the absence of monomer. Yet, additional experiments evidenced that 1-hexene polymerization catalyzed by the {Cp/Flu}-type zirconocene complexes could be reactivated by introduction of dihydrogen as chain-transfer agent, and also of ethylene, a smaller, much more reactive monomer.

The intrinsic differences between the {SBI}- and {Cp/Flu}-type zirconocene polymerization systems, showcasing dissimilar propensities towards deactivation, were investigated by analyzing high-resolution ¹³C NMR data obtained for the corresponding poly(propylene-co-ethylene) samples. The formation of "dormant" Zr-sec-alkyl species by 2,1-misinsertion of the α -olefin appeared to have a critical role for deactivation process. The corresponding species in the case of the {SBI}-based systems are still reactive and can either further propagate or regenerate an active hydrido species upon β -H elimination. On the other hand, for the {Cp/Flu}-based systems, the Zr-sec-alkyl species, although being much less frequent than for the {SBI}-based systems (0.02 vs 0.36 mol%, respectively), appeared to be exceptionally reluctant to further propagation.

Thus, overall, the kinetic data obtained in these studies indicated just a slightly inferior activation efficiency for {Cp/Flu}-type precatalysts (1–12%) as for the overall more productive {SBI}-type precatalysts (4–18%) under identical conditions. Noteworthy, the propagation rate constants k_p for 1-hexene polymerization reactions catalyzed by {Cp/Flu}-based systems are at least one order larger than those for the {SBI}-type catalysts. However, the {Cp/Flu} systems appear to undergo infrequent but irreversible deactivation by 2,1-misinsertion of the α -olefin, while {SBI} systems are not impacted (in terms of propagation) by these misinsertions, although they are more frequent.

4. Summary

Despite the apparent maturity and important industrial accomplishments of metallocene polymerization catalysis, it still remains challenges in this field to develop ever more efficient

catalysts and to produce polyolefinic materials with predefined and tailored properties for ever evolving and always more demanding commercial applications. In order to address these demands timely, the development of new metallocene-based polymerization systems and innovative processes is still being pursued.

In this account, we reported on our continuing endeavors to ameliorate an ubiquitous family of isoselective propylene polymerization catalysts based on C_1 -symmetric group 4 *ansa*-metallocenes incorporating multi-substituted {Cp/Flu} ligands. Much structural information was collected for neutral metallocenes, including many new ones, as well as rare solution dynamics and reorganization mechanisms for the derived thereof metallocenium ion-pairs.

Overall, it appears that the polymerization activity of catalytic systems can be correlated to the higher stability of the active species generated. The latter is determined by numerous independent factors, including sensitiveness of cations toward various deactivation processes, metallocenium-anion ion-pairing strength, and propensity of the given ionic intermediates to interact *e.g.* with aluminum alkyls. Kinetic studies, applied for investigating the activation mechanism, allowed us to evaluate the activation efficiency of the {Cp/Flu}-type metallocene systems, revealing their unexpected apparent superiority over the {SBI}-type analogues in terms of intrinsic propagation rates. However, monomer 2,1-misinsertions, resulting in decay of active sites via formation of dormant M-sec-alkyl species, were evidenced. Most importantly, these seem to be exceptionally deleterious for the {Cp/Flu}-based catalysts, in contrast to {SBI}-type analogues. Yet, the dormant M-sec-alkyl species resulting from these 2,1-misinsertions can be efficiently reactivated by introduction of small molecules (H_2 or ethylene), affording a simple "solution" easy to implement on the industrial scale.

Acknowledgements

We thank Total Petrochemicals and Total S.A. for longstanding financial support. We are also very grateful to the dedicated students who have been involved in this research program: Dr. Nicolas Marquet, Dr. Manuela Bader, Dr. Gabriel Theurkauff, Dr. Ludovic Castro, Dr. Fabien Proutiere, Dr. Gilles Schnee, Dr. Lars Jende, Dr. Orlando Santoro, Dr. Thierry Chavagnan, Dr. Abdallah Zeineddine and Dr. Xavier Desert. We wish to thank our past and current industrial partners: Dr. Abbas Razavi, Mr. Vincenzo Belia, Dr. David Ribour, Dr. Christian Lamotte, Dr. Katty Den Dauw, Dr. Olivier Lhost, Dr. Luc Haspeslagh, Dr. Jerome Waassenaar, Dr. Armelle Sigwald, Dr. Pierre Boulens, Dr. Thomas Coustham, Dr. Virginie Cirriez, Dr. Pierre Giusti, Dr. Olivier Miserque, Dr. Aurelien Vantomme, Dr. Jean-Michel Brusson, Dr. Sophie Bire, Dr. Alvaro Fernandez, Dr. Alexandre Welle for stimulating discussions and sharing their extensive industrial expertise. We also thank our academic collaborators: Prof. Laurent Maron (LPCNO, INSA Toulouse) for his assistance in DFT analysis and Prof. John A. Gladysz (Texas A&M University) for co-supervising a part of this work.

1 **Keywords:** metallocenes • polymerization • polyolefins • ion-
2 pairs • active species

3
4
5
6
7
8
9
10
11
12
13
14
15
16
17
18
19
20
21
22
23
24
25
26
27
28
29
30
31
32
33
34
35
36
37
38
39
40
41
42
43
44
45
46
47
48
49
50
51
52
53
54
55
56
57
58
59
60
61
62
63
64
65

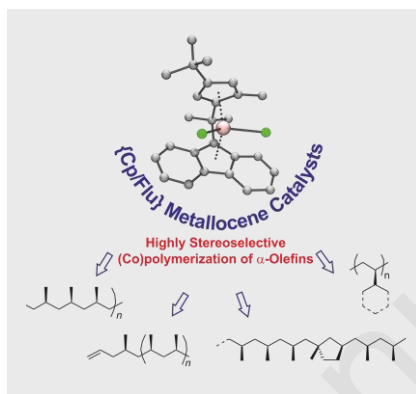
Accepted manuscript

Entry for the Table of Contents (Please choose one layout)

Layout 1:

PERSONAL ACCOUNT

This personal account summarizes our continuing endeavors to advance the family of industry-relevant stereoselective propylene polymerization catalysts based on C_1 -symmetric group 4 *ansa*-metallocenes incorporating multi-substituted fluorenyl-cyclopentadienyl {Cp/Flu} ligands.



Evgueni Kirillov* and Jean-François Carpentier*

Page No. – Page No.

{Cyclopentadienyl/Fluorenyl}-Group 4 *ansa*-Metallocene Catalysts for Production of Tailor-Made Polyolefins

References

- [1] (a) Metallocene Catalyzed Polymers: Materials, Properties, Processing and Markets. (Eds. G. M. Benedikt, B. L. Goodall), Plastic Design Library, William Andrew Inc., Norvich, NY, 1999, pp 1–386; (b) Metalorganic Catalysts for Synthesis and Polymerization. Recent Results by Ziegler-Natta and Metallocene Investigations. (Ed. W. Kaminsky) Springer-Verlag, Berlin, Heidelberg, New York, 1999, pp 1–674.
- [2] (a) J. A. Gladysz, Special issue: Frontiers in Metal-Catalyzed Polymerization, *Chem. Rev.* **2000**, *100*, 1167–1168; (b) Resconi, L.; Fritze, C. in *Polypropylene Handbook* (Ed.: Pasquini, N.), Hanser Publishers, Munich, 2005, pp 107–147; (c) Fink, G.; Brintzinger, H. H. in *Metal-Catalysis in Industrial Organic Processes* (Eds. Chiusoli, G. P.; Maitlis, P. M.), Royal Society of Chemistry, Colchester, 2006, pp 218–254; (d) H. Alt, Special issue: Metallocene complexes as catalysts for olefin polymerization, *Coord. Chem. Rev.* **2006**, *250*, 1; (e) Kaminsky, W. *Macromolecules* **2012**, *45*, 3289–3297.
- [3] M. Sturzel, S. Mihan, R. Mulhaupt, *Chem. Rev.* **2016**, *116*, 1398–1433.
- [4] A. H. Tullo, in *Metallocenes Rise Again*. *C&EN* **2010**, *88*, 10–16.
- [5] K. Patel, S. H. Chikkali, S. Sivaram, *Prog. Polym. Sci.* **2020**, *109*, 101290.
- [6] (a) H. G. Alt, E. Samuel, *Chem. Soc. Rev.*, **1998**, *27*, 323–329; (b) H. G. Alt, A. Koppl, *Chem. Rev.* **2000**, *100*, 1205–1221.
- [7] (a) J. A. Ewen, R. L. Jones, A. Razavi, J. D. Ferrara, *J. Am. Chem. Soc.* **1988**, *110*, 6255–6256. (b) J. A. Ewen, M. J. Elder, R. L. Jones, L. Haspelslagh, J. L. Atwood, S. G. Bott, K. Robinson, *Makromol. Chem., Macromol. Symp.* **1991**, *49/49*, 253–295; (c) A. Razavi, U. Thewalt, *Coord. Chem. Rev.* **2006**, *250*, 155–169; (d) A. Razavi, V. Bellia, D. Baekelmans, M. Slawinsky, S. Sirol, L. Peters, U. Thewalt, *Kinetics and Catalysis*, **2006**, *47*, 257–267;
- [8] (a) M. C. Chen, T. J. Marks, *J. Am. Chem. Soc.* **2001**, *123*, 11803–11804; (b) C. Zuccaccia, N. G. Stahl, A. Macchioni, M.-C. Chen, J. A. Roberts, T. J. Marks, *J. Am. Chem. Soc.* **2004**, *126*, 1448–1464; (c) M. C. Chen, J. A. Roberts, T. J. Marks, *Organometallics* **2004**, *23*, 932–935; (d) M. C. Chen, J. A. Roberts, T. J. Marks, *J. Am. Chem. Soc.* **2004**, *126*, 4605–4625; (e) M. C. Chen, J. A. S. Roberts, A. M. Seyam, L. Li, C. Zuccaccia, N. G. Stahl, T. J. Marks, *Organometallics* **2006**, *25*, 2833–2850; (f) J. S. A. Roberts, M.-C. Chen, A. M. Seyam, L. Li, C. Zuccaccia, N. G. Stahl, T. J. Marks, *J. Am. Chem. Soc.* **2007**, *129*, 12713–12733.
- [9] (a) S. A. Miller, J. E. Bercaw, *Organometallics* **2002**, *21*, 934–945; (b) S. A. Miller, J. E. Bercaw, *Organometallics* **2004**, *23*, 1777–1789; (c) S. A. Miller, J. E. Bercaw, *Organometallics* **2006**, *25*, 3576–3592
- [10] (a) C. Alonso-Moreno, S. J. Lancaster, C. Zuccaccia, A. Macchioni, M. Bochmann, *J. Am. Chem. Soc.* **2007**, *129*, 9282–9283; (b) C. Alonso-Moreno, S. J. Lancaster, J. A. Wright, D. L. Hughes, C. Zuccaccia, A. Correa, A. Macchioni, L. Cavallo, M. Bochmann, *Organometallics* **2008**, *27*, 5474–5487.
- [11] (a) L. Resconi, C. Fritze, *Polypropylene Handbook* (Ed.: N. Pasquini), Hanser Publishers, Munich, **2005**, pp 107–147; (b) W. Kaminsky, *Macromolecules* **2012**, *45*, 3289–3297; (c) G. Fink, H. H. Brintzinger, *Metal-Catalysis in Industrial Organic Processes* (Eds.: G. P.; Chiusoli, P. M. Maitlis), Royal Society of Chemistry, Colchester, **2006**, pp 218–254; (d) A. Razavi, *C. R. Acad. Sci., Chemistry* **2000**, *3*, 615–625.
- [12] E. Kirillov, S. Kahlal, T. Roisnel, T. Georgelin, J.-Y. Saillard, J.-F. Carpentier, *Organometallics* **2008**, *27*, 387–393.
- [13] E. Kirillov, S. Kahlal, J.-Y. Saillard, J.-F. Carpentier, *Coord. Chem. Rev.* **2005**, *249*, 1221–1248.
- [14] J. H. Day, *Chem. Rev.* **1953**, *53*, 167–189.
- [15] (a) E. Kirillov, N. Marquet, A. Razavi, V. Belia, F. Hampel, T. Roisnel, J. A. Gladysz, J.-F. Carpentier, *Organometallics* **2010**, *29*, 5073–5082; (b) E. Kirillov, J. A. Gladysz, A. Razavi, (Friedrich-Alexander Universität Erlangen-Nürnberg and Atofina), *Eur. Pat. Appl.* **2005**, EP 05105162.1 (13/06/2005). (c) J.-F. Carpentier, E. Kirillov, A. Razavi, (Université de Rennes 1 and Total Petrochemicals), *Eur. Pat. Appl.* **2006**, EP 06121181.9 (25/09/2006).
- [16] (a) E. Kirillov, N. Marquet, M. Bader, A. Razavi, V. Belia, F. Hampel, T. Roisnel, J. A. Gladysz, J.-F. Carpentier, *Organometallics* **2011**, *30*, 263–272; (b) J.-F. Carpentier, E. Kirillov, N. Marquet, A. Razavi, (Université

- de Rennes 1 and Total Petrochemicals), Eur. Pat. Appl. **2010**, EP 2204375 A1 20100707.
- [17] (a) M. Bader, N. Marquet, E. Kirillov, T. Roisnel, A. Razavi, O. Lhost, J.-F. Carpentier, *Organometallics* **2013**, *32*, 8375–8387; (b) J.-F. Carpentier, E. Kirillov, N. Marquet, A. Razavi, (Université de Rennes 1 and Total Petrochemicals), Eur. Pat. Appl. **2010**, EP 2196481 A1 20100616; (c) M. Bader, J.-F. Carpentier, E. Kirillov, O. Lhost, D. Ribour, (Université de Rennes 1 and Total Petrochemicals), PCT Int. Appl. **2013**, WO 2013060810 A1 20130502; (d) M. Bader, J.-F. Carpentier, E. Kirillov, O. Lhost, C. Lamotte, K. Den Dauw, (Université de Rennes 1 and Total Petrochemicals), PCT Int. Appl. **2015**, WO 2015082709 A1 20150611.
- [18] The SambVca 2.1 software was used to calculate % V_{bur} and generate steric maps: L. Falivene, Z. Cao, A. Petta, L. Serra, A. Poater, R. Oliva, V. Scarano, L. Cavallo, *Nat. Chem.* **2019**, *11*, 872–879.
- [19] (a) L. J. Irwin, J. H. Reibenspies, S. A. Miller, *Polyhedron*, **2005**, *24*, 1314–1324; (b) D. Drago, P. S. Pregosin, A. Razavi, *Organometallics* **2000**, *19*, 1802–1805.
- [20] Ionic radii for six-coordinate metal centers, Hf^{4+} : 0.71 Å vs. Zr^{4+} : 0.72 Å, see: R. D. Shannon, *Acta Cryst.* **1976**, *A32*, 751–767.
- [21] Results reported by other groups for similar {Cp/Flu}-based systems were not included in the discussion, since they were obtained under different polymerization conditions.
- [22] However, these data should be considered with care, since the polymerization reactions carried out with the reference {SBI}-1 (and other highly active systems such as that based on the V-PhH-like platform) were quite exothermic, even with low precatalyst loadings. As a result, the temperature of the reaction mixtures could hardly be controlled, often outreaching configured values after a few minutes.
- [23] V. Busico, R. Cipullo, C. Pellecchia, G. Talarico, A. Razavi, A. *Macromolecules* **2009**, *42*, 1789–1791.
- [24] (a) L. Resconi, I. Camurati, O. Sudmeijer, *Top. Catal.* **1999**, *7*, 145–163; (b) C. Janiak, *Coord. Chem. Rev.* **2006**, *250*, 66–94.
- [25] (a) W. Weng, W. Hu, A. H. Dekmezian, C. J. Ruff, *Macromolecules* **2002**, *35*, 3838–3843; (b) O. Santoro, L. Piola, K. Mc Cabe, O. Lhost, K. Den Dauw, A. Vantomme, A. Welle, L. Maron, J.-F. Carpentier, E. Kirillov, *Macromolecules* **2020**, *20*, 8847–8857.
- [26] Dong, J.-Y.; Hu, Y. *Coord. Chem. Rev.* **2006**, *250*, 47–65.
- [27] M. R. Kesti, R. M. Waymouth, *J. Am. Chem. Soc.* **1992**, *114*, 3565–3567.
- [28] M. Bader, G. Theurkauff, K. Den Dauw, C. Lamotte, O. Lhost, E. Kirillov, J.-F. Carpentier, *Polymer Chem.* **2014**, *5*, 5560–5568.
- [29] G. Theurkauff, K. Den Dauw, O. Miserque, A. Vantomme, J.-M. Brusson, J.-F. Carpentier, E. Kirillov, *Polyolefins J.* **2017**, *4*, 123–136.
- [30] (a) T. Yoshida, N. Koga, K. Morokuma, K. *Organometallics* **1996**, *15*, 766–777; (b) A. Laine, B. B. Coussens, J. T. Hirvi, A. Berthoud, N. Friederichs, J. R. Severn, M. Linnolahti, M. *Organometallics* **2015**, *34*, 2415–2421; (c) M. S. Kuklin, V. Virkkunen, P. M. Castro, L. Resconi, M. Linnolahti, M. *Eur. J. Inorg. Chem.* **2015**, 4420–4428.
- [31] L. Boggioni, M. Cornelio, S. Losio, A. Razavi, I. Tritto, I. *Polymers* **2017**, *9*, 581–598.
- [32] (a) L. Castro, E. Kirillov, O. Miserque, A. Welle, L. Haspeslagh, J.-F. Carpentier, L. Maron, *ACS Catal.* **2015**, *5*, 416–425; (b) L. Castro, G. Theurkauff, A. Vantomme, A. Welle, L. Haspeslagh, J.-M. Brusson, L. Maron, J.-F. Carpentier, E. Kirillov, *Chem. Eur. J.* **2018**, *24*, 10784–10792.
- [33] (a) M. Bochmann, *Organometallics* **2010**, *29*, 4711–4740; (b) M. Bochmann, *J. Organomet. Chem.* **2004**, *689*, 3982–3998; (c) J.-N. Pedetour, K. Radhakrishnan, A. Deffieux, *Macromol. Rapid Commun.* **2001**, *22*, 1095–1123.
- [34] E. Y.-X. Chen, T. J. Marks, *Chem. Rev.* **2000**, *100*, 1391–1434.
- [35] (a) K. P. Bryliakov, D. E. Babushkin, E. P. Talsi, A. Z. Voskoboinikov, H. Gritzo, L. Schroder, H.-R. H. Damrau, U. Wieser, F. Schaper, H. H. Brintzinger, *Organometallics* **2005**, *24*, 894–904; (b) K. P. Bryliakov, N. V. Semikolenova, V. N. Panchenko, V. A. Zakharov, H.-H. Brintzinger, E. P. Talsi, *Macromol. Chem. Phys.* **2006**, *207*, 327–225; (c) O. Y. Lyakin, K. P. Bryliakov, V. N. Panchenko, N. V. Semikolenova, V. A. Zakharov, E. P. Talsi, *Macromol. Chem. Phys.* **2007**, *208*, 1168–1175.
- [36] A. Valente, A. Mortreux, M. Visseaux, P. Zinck, *Chem. Rev.* **2013**, *113*, 3836–3857.
- [37] (a) G. Theurkauff, M. Bader, N. Marquet, A. Bondon, T. Roisnel, J.-P. Guegan, A. Amar, A. Boucekkine, J.-F. Carpentier, E. Kirillov, E. *Organometallics* **2016**, *35*, 258–276; (b) G. Theurkauff, A. Bondon, V. Dorcet, J.-F. Carpentier, E. Kirillov, E. *Angew. Chem. Int. Ed.* **2015**, *127*, 6343–6346; *Angew. Chem.* **2015**, *127*, 6441–6444.
- [38] G. Theurkauff, T. Roisnel, J. Waassenaar, J.-F. Carpentier, E. Kirillov, E. *Macromol. Chem. Phys.* **2014**, *215*, 2035–2047.
- [39] X. Desert, J.-F. Carpentier, E. Kirillov, E. *Coord. Chem. Rev.* **2019**, *386*, 50–68.
- [40] X. Desert, P. Proutiere, A. Welle, K. Den Dauw, A. Vantomme, O. Miserque, J.-M. Brusson, J.-F. Carpentier, E. Kirillov, E. *Organometallics* **2019**, *38*, 2664–2673.
- [41] F. Ghiotto, C. Pateraki, J. R. Severn, N. Friederichs, M. Bochmann, M. *Dalton Trans.* **2013**, *42*, 9040–9048.



Click here to access/download

Supporting Information

Manuscript_tcr.202000142_revised_SI_reviewonly.docx





Click here to access/download
Additional Material - Author
Response_Letter_tcr.202000142.pdf

